AN ABSTRACT OF THE DISSERTATION OF

Angela Doneanu for the degree of Doctor of Philosophy in Chemistry
presented on April 28, 2005.
Title: Monolithic Sorbents for Microscale Separations

Abstract approved:

Redacted for Privacy

Vincent T. Remcho

Over the last decade, the miniaturization of analytical systems has become an increasingly important and interesting research area. Miniaturized systems offer many advantages, including reduced reagent and sample consumption, shorter analysis times, portability and disposability. This dissertation describes novel approaches in this direction, focusing on two areas: the miniaturization of existing column chromatographic systems and the development of microfluidic systems in which the separation is performed in a channel on a microchip.

A new type of methacrylate-based monolithic capillary columns for liquid chromatography and capillary electrochromatography were prepared within the confines of fused-silica tubing using Starburst dendrimers to affect porosity. The polyamidoamine (PAMAM) dendrimers were incorporated into a solution of functionalized monomer, cross-linker, solvents, and polymerization initiator. Thermal polymerization, followed by the removal of solvent and dendrimers,

produced a continuous rod of polymer with uniform porosity. Different column porosities were obtained by varying the amount of the dendrimer template. The chromatographic performance of these monolithic columns was evaluated using a peptides mixture obtained by tryptic digestion of chicken egg lysozyme.

A distinct advantage of polymer monolithic stationary phases over conventional packed chromatographic beds is the ability to prepare them easily and rapidly via free radical polymerization within the channels of a microfluidic device.

In this work, continuous polymeric beds were prepared within a channel of three different microchip substrates: glass, poly(dimethylsiloxane) and polycarbonate. The methacrylate-based monolith was cast *in-situ* via UV-initiated polymerization. The functionalization of the inner wall of the channel with methacryloyl groups enabled the covalent binding of the monolith to the wall. The morphology of the wall-anchored monolith was studied by SEM of chip sections, and by SEM of an extruded segment of non-anchored monolith from a separate chip.

Monolithic Sorbents for Microscale Separations

by

Angela Doneanu

A DISSERTATION

submitted to

Oregon State University

in partial fulfillment of
the requirements for the
degree of

Doctor of Philosophy

Presented on April 28, 2005
Commencement June 2005

Doctor of Philosophy dissertation of Angela Doneanu presented on April 28, 2005.

APPROVED:

Redacted for Privacy

Major Professor, representing Chemistry

Redacted for Privacy

Chair of the Department of Chemistry

Redacted for Privacy

Dean of Graduate School

I understand that my dissertation will become part of the permanent collection of Oregon State University libraries. My signature below authorizes release of my dissertation to any reader upon request.

Redacted for Privacy

Angela Doneanu, Author

ACKNOWLEDGMENTS

First I want to express my gratitude to my adviser, Dr. Vincent Remcho, who provide my with his knowledge, guidance and continuous support during my graduate school experience. I have benefited both professionally and personally from his mentoring.

I would also like to thank my committee members: Dr. James Ingle, Dr. Michael Lerner, Dr. Claudia Maier and Dr. Gregory Rorrer for offering the academic guidance that I needed to complete my program at Oregon State University.

My thanks go to many collaborators including Dr. Alex Chang (Dept. of Chemical Engineering), Dr. Brian Paul (Dept. of Industrial and Manufacturing Engineering), Dr. Skip Rochefort (Dept. of Chemical Engineering), Dr. Tom Plant, Dr. Lioubov Kabalnova, Al Soeldner, Dr. Catalin Doneanu (Univ. of Washington) for allowing use of their facilities and providing expertise, without which crucial data would have not been attainable.

Additionally, I want to acknowledge the following people that I have been fortunate to work alongside at some time during the course of this research: Gabriela Chirica, Patrick Vallano, Stacey Clark, Carlos Gonzalez, Jack Rundel, Laura Lessard, Dana Hutanu, Myra Koesdjojo, and Yolanda Tennico.

I would like to thank my family and friends for their support of me moving halfway around the world to pursue my dreams.

Lastly and most importantly I wish to thank my husband Catalin for his love, encouragement, patience and support in my determination to find and realize my potential. With him I am more than I ever could be on my own. Thank you.

TABLE OF CONTENTS

TABLE OF CONTENTS (Continued)

TABLE OF CONTENTS (Continued)

Page

TABLE OF CONTENTS (Continued)

LIST OF FIGURES

LIST OF FIGURES (Continued)

Figure Page

LIST OF FIGURES (Continued)

Figure Page

LIST OF TABLES

Table Page

MONOLITHIC SORBENTS FOR MICROSCALE SEPARATIONS

CHAPTER 1

INTRODUCTION

Miniaturized separation techniques have become very attractive because they offer a number of advantages over classical methods: for example, reduced chemical consumption, separation improvement, and enhanced sensitivity. It is also very advantageous that they require minute sample volumes, which is very often of primary importance in the biomedical sciences. At present, two main trends in miniaturization of separation systems can be observed. The first is miniaturization of existing column chromatographic systems. The second is development of microfluidic systems in which the separation is performed in a channel on a microchip.

This thesis treats both aspects of miniaturization and is organized as follows: The first aim of Chapter 1 is to introduce the theoretical aspects of capillary electrochromatography (CEC). This chapter also describes the design and operation of CEC instrumentation. The focus of discussion is on the column, the "heart" of any separation system. An overview of the most widely utilized column technologies, with emphasize on monolithic columns is also presented.

The second chapter describes the basic manufacturing processes for both glass and plastic microfluidic devices fabrication. A summary of common injection methods

is included, along with a brief description of the most frequently used detection scheme, laser induced fluorescence.

In Chapter 3, I investigate new monolithic stationary phases that afford control over porosity and, to a certain degree, over the surface chemistry of the sorbent. The novelty of this study lies in the use of dendrimers for generation of uniform pore structures. Different column porosities can be obtained by varying the amount of the dendrimer template as evidenced by electron microscopy and mercury intrusion porosimetry. The effect of dendrimer concentration on chromatographic performance is studied in detail.

Our group is currently involved in developing high-throughput nanoextraction technology for implementation in microsystems. The first step toward this objective was to evaluate the feasibility of transferring available separation techniques into microchip format. In Chapter 4, the use of electrophoresis to separate species in channels within glass chips is examined.

The main goal of the research presented in Chapter 5 was to develop a surface modification method that makes possible the anchoring of polymeric monoliths to the walls of the microchip.

1.1. Capillary electrochromatography

Capillary electrochromatography (CEC) has enjoyed a high level of interest and rapid development in the past decade, leading to a quickly growing number of publications in this field. CEC is a chromatographic separation method in which the liquid mobile phase is driven through a stationary phase by electroosmotic flow (EOF) using a high electric field. One of the primary reasons for interest in this technique is the mixed separation mechanism of CEC that is borrowed from both high-performance liquid chromatography (HPLC) and capillary zone electrophoresis (CZE). Retention in CEC is based on solute partitioning between the mobile and stationary phases. Charged solutes can also migrate via electrophoresis as well, providing a multimechanistic retention scheme.

The history of CEC can be traced back to 1974 when Pretorius et al. suggested the use of EOF as a pumping mechanism alternative to pressure driven flow [1]. The viability of CEC in packed columns was demonstrated by Jorgenson and Lukacs in 1981 [2] who reported the separation of 9-methylanthracene from perylene on a 170μm i.d. capillary packed with 10μm reversed-phase packing material. Although the efficiencies were relatively low (~60,000 plates/m) the principle of electrically driven chromatography using small diameter particles was proven. It was, however, the pioneering theoretical and practical approach of Knox and Grant in 1987 [3] that finally resurrected interest in CEC.

1.2. Electroosmotic flow

The driving force in electroseparation methods results from the electrical double layer that exists at the liquid-solid interface between, in case of CZE, the bulk liquid and the capillary surface and in CEC the packing material and mobile phase, as is illustrated in **Figure 1.1.**

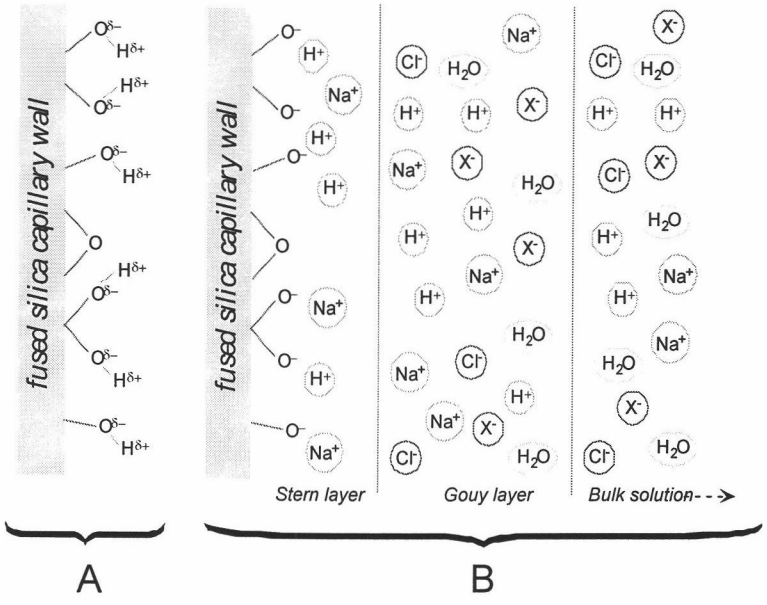

Figure 1.1. Schematic representation of the electrical double layer near the surface of fused silica capillary tubing. Adapted from reference [4].

Under alkaline conditions, the surface silanol groups of the fused silica will become ionized leading to a negatively charged surface. The distribution of nearby ions in solution is affected, and counterions are attracted to the surface to maintain electroneutrality. An electrochemical double layer is formed. Ions closest to the wall are tightly bound and relatively immobile, even under the influence of an electric field. This layer of ions is called the Stern layer. Further from the wall is a compact and mobile region with substantial cationic character. This diffuse outer region is known as the Gouy layer.

The formation of the electrical double layer gives rise to a potential that varies as a function of distance from the capillary wall (or particle surface). This relationship is indicated in **Figure 1.2.** , in which potential (ψ) versus distance is plotted.

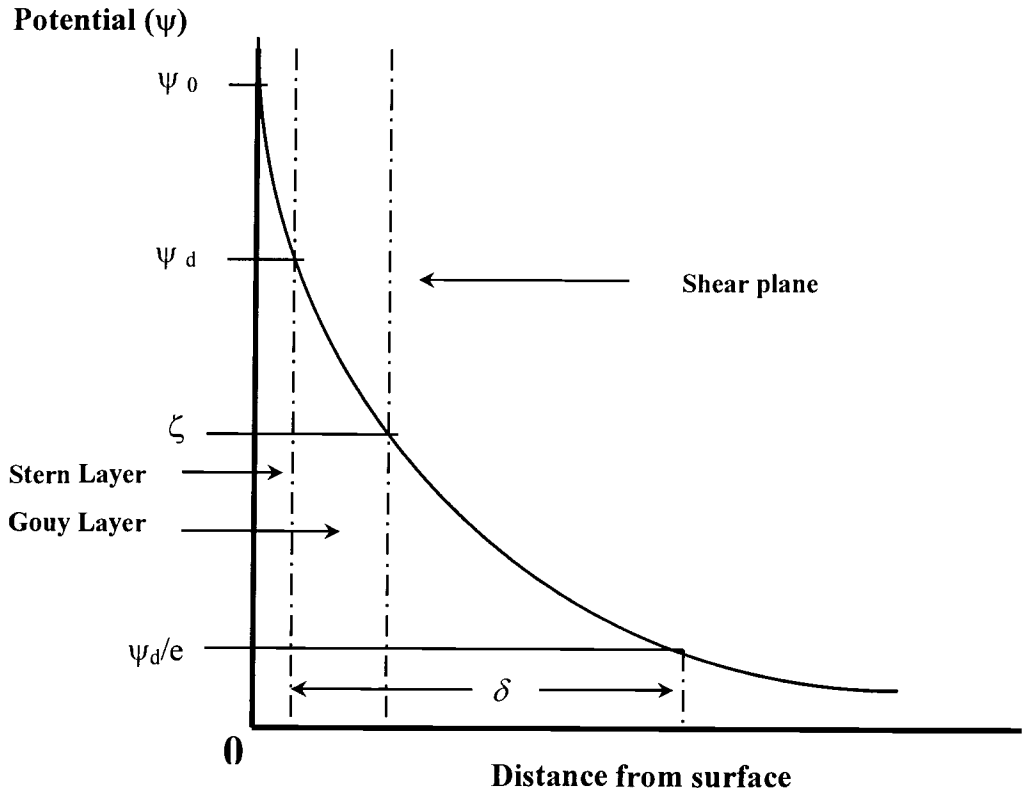

Figure 1.2. Potential as a function of distance from a charge surface. The potential at the plane of shear is the zeta potential ζ. The distance over which the potential at the boundary of the Stern and Gouy layers, ψ_d, decays by a factor of $1/e$ is known as the double layer thickness, δ. Adapted from reference [5].

The electrical potential drop between the silica wall and the surface of shear (that separates the counterions not free to exchange with the bulk solution from the mobile counterions) is termed the zeta potential, ζ, and falls exponentially in the

diffuse layer eventually to zero, but by a factor e^{-1} over a distance δ, known as the double layer thickness. The zeta potential depends on the product of δ and the surface charge σ according to [6]:

$$\zeta = \frac{\sigma\delta}{\varepsilon_o \varepsilon_r} \tag{1.1}$$

where ε_0 is the vacuum permittivity, and ε_r is the dielectric constant of the electrolyte solution. The double layer thickness also depends on ε_r and on C, the molar concentration of the electrolyte solution [3]:

$$\delta = \left(\frac{\varepsilon_o \varepsilon_r RT}{2CF^2} \right)^{1/2} \tag{1.2}$$

Typical values of δ for a monovalent electrolyte are nominally δ = 10 nm for a 1 μM solution and δ = 1 nm for a 100 μM solution.

When a potential difference is applied across the column length, the solvated cations in the diffuse layer move towards the cathode, and because of enormous friction between species in solution will drag the surrounding bulk solution along with them. The resulting electroosmotic mobility, μ_{eof} is then related to ζ and to η the viscosity of the solution by:

$$\mu_{eof} = \frac{\varepsilon_0 \varepsilon_r \zeta}{\eta} \qquad (1.3)$$

and the linear velocity, u_{eof}, is described by:

$$u_{eof} = \frac{\varepsilon_0 \varepsilon_r \zeta E}{\eta} \qquad (1.4)$$

where E is the electric field strength.

This equation is applicable in the absence of double layer overlap and shows that unlike the flow profile in pressure-driven flow, which is parabolic, the flow profile in electroosmotic flow is essentially flat over the cross-sectional area of the capillary. **Figure 1.3.** shows an idealized view of the axial profiles of pressure and electrically driven flow.

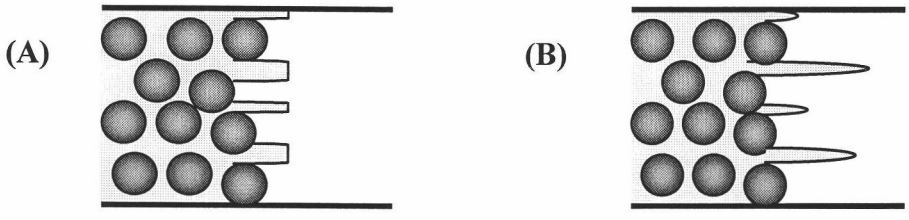

Figure 1.3. Schematic representation of electroosmotic (A) and pressure-driven (B) flow profiles in a packed CEC column.

The phenomenon of electroosmotic flow has been exploited in the past several years in the capillary format in CEC, due to more efficient heat transfer. Its intrinsically flat flow profile generates high efficiencies, to date comparable only to those of capillary gas chromatography. EOF controls the migration velocities of neutral analytes; in the case of charged compounds the total velocity is an additive function of electroosmotic and electrophoretic mobility. Simultaneously, chromatographic retention specific to HPLC is superimposed on the electro-driven transport typical of CE. Just as in μHPLC, a wide selectivity range is available and can be finely tuned by using mixtures of organic solvents and aqueous buffers. Mobile-phase additives, such as ion-pairing reagents, surfactants, and crown ethers, can further enhance selectivity opening the door for more applications.

Driving the flow by electroosmosis results in a number of advantages for CEC over HPLC. Since the EOF is independent of the size of the particles in the packed bed, in contrast to HPLC, smaller particles and longer columns may be employed with consequent increase in column efficiency and resolution. A further advantage of electrodriven flow is that the velocity profile of the EOF reduces dispersion of the band of solute passing through the column, with further improvement in column efficiency.

1.3. Instrumentation for Capillary Electrochromatography

In principle, commercial or homemade equipment for capillary electrophoresis is sufficient to execute CEC. In its simplest form, a CEC instrument includes the following basic components: a high-voltage power supply, a column or a microfluidic channel in which an EOF is generated and electrochromatographic separation processes take place, two buffer reservoirs that can accommodate both the capillary and the electrodes connected to the power supply, and a detection device. Thermostatting of the capillary is critical to achieve efficient and reproducible separations and, hence, some type of capillary thermostatting system should be used. However, one modification typical of commercial CE equipment is the pressurization of the solvent reservoirs. There is a general consensus that pressurization at inlet and/or outlet ends of the CEC column is needed to prevent formation of bubbles.

A schematic of the instrumentation is shown in **Figure 1.4.** Application of an electric field along the capillary axis results in bulk flow of the mobile phase by electroosmosis. The ionic species in the sample plug migrate with an electrophoretic mobility (direction and velocity) determined by their charge and mass.

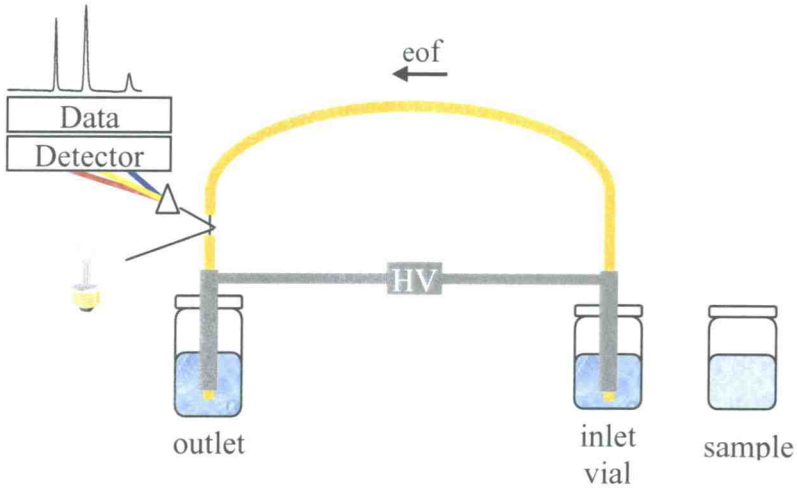

Figure 1.4. CEC instrumentation

1.4. Column technology

The separation column is the most important element of any chromatographic system. The attainable resolving power of the system, the efficiency of the separation, and in the case of CEC the velocity of the mobile phase are decided by the nature of the column. A wide variety of approaches are currently being explores in the fabrication and innovation of columns for capillary electrochromatography.

In this section, a summary of the most widely utilized column technologies, including packed columns, open tubular columns and monolithic columns will be presented.

1.4.1. Packed columns

Originally, CEC employed the same type of columns as μHPLC, namely, conventional HPLC silica based particles packed into fused silica capillaries. Porous plugs attached to the fused silica walls, also known as frits, hold the sorbent material within the confines of the capillary tubing.

Different techniques have been proposed for the preparation of packed capillary columns, including dry packing, slurry packing, supercritical fluid packing, or electrokinetic packing. The aim of the packing process is to fill the capillary with the sorbent particles to obtain a homogeneous and stable bed of the stationary phase.

The slurry packing technique has been used most frequently because it builds on a broad base of experience with the packing of conventional size columns. The concept of slurry packing, illustrated in **Figure 1.5.** , relies on the preparation of packing material suspension in an appropriate solvent and introducing it into a column under pressure.

The fabrication of retaining frits as well as the subsequent packing of the particles requires considerable experimental skill in order to obtain stable and reproducible columns.

Just as in μHPLC, frit fragility can significantly decrease the lifetime of the column. Moreover, nonspecific interactions occurring at the surface of the frits, differential flow at the interface between frits and the chromatographic bed, and, most

important, the lack of reproducible frit fabrication procedures have a deleterious effect on column-to-column reproducibility.

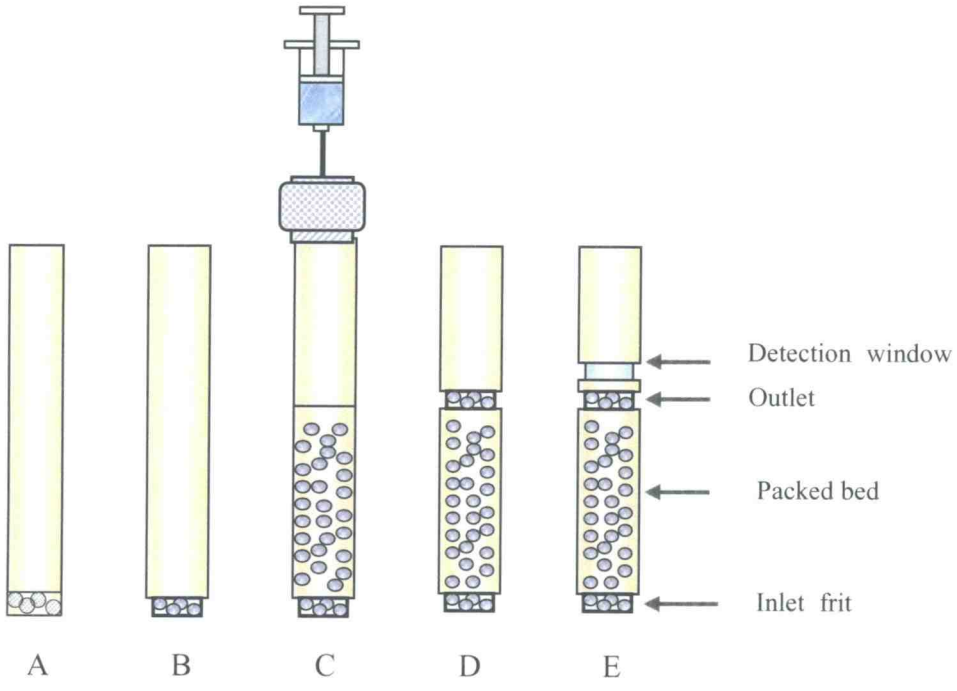

Figure 1.5. Schematic representation of the slurry packing procedure. (A) tapping empty column into dry packing material until the material protruded a short distance, (B) formation of the frit: the packing material is sintered by heating with an electric arc fusion splicer, (C) force the slurry into the column upon application of pressure, (D) prepare the outlet frit, while the packed bed is still pressurized and (E) prepare the detection window downstream from the outlet frit.

The technical difficulties associated with packed columns have spurred the development of a number of different approaches for column fabrication, such as open-tubular columns, entrapped packed columns and polymeric monolithic columns.

1.4.2. Open-tubular CEC

In open-tubular (OT) columns the capillary wall is activated and subsequently treated to generate a polymeric coating, molecular monolayer or porous layer of stationary phase. Tan and Remcho developed the first OT CEC polymer coatings in 25 μm i.d. capillaries. The polymethacrylate coatings provided a hydrophobic surface, which promoted the separation of benzoates with efficiency greater than 250,000 plates/m [7]. Later, the same authors extended the technology to the synthesis of a porous layer of molecularly imprinted polymer for the separation of D and L isomers of dansyl phenylalanine [8]. To date, several types of organic modifiers, including octadecyl, diol, cholestryl, and chiral selectors, have been attached to etched capillary surfaces and tested in the OT CEC format [9]. The main advantage of OT CEC is that separation efficiency can be doubled using this type of column. The trade-off is that the OT columns can easily be overloaded and therefore require a sensitive detection system. As a consequence, the range of practical applications is somewhat limited.

1.4.3. Monolithic Columns.

A viable alternative to packed capillary CEC has been offered by fritless monolithic columns. A monolithic column was defined as "a continuous unitary porous structure prepared by in situ polymerization or consolidation inside the column tubing and, if necessary, the surface is functionalized to convert it into a sorbent with the desired chromatographic binding properties" [10]. While quite general, this definition actually covers a range of methods that can be used to produce continuous bed columns. The many reported methodologies for producing monolithic columns published to date differ in their manufacturing process and the end-product monolith.

1.4.4. Entrapped packed columns

Monoliths can be prepared by converting a conventionally packed column into a monolithic structure. Monolithic columns from particles are designed to inherit the versatility of well-developed particulate media but avoid the end-frits and instability of packed columns. Various methods for preparing monoliths from particles are reviewed in the following section.

Asiaie et al. [11] described the preparation of particle-sintered monoliths in which the reverse-phase silica particles packed in a fused silica capillary were sintered together and to the capillary inner wall through a thermal treatment. Due to the harsh experimental conditions used in the sintering process, the stationary phase was

destroyed, and thus, post deactivation and functionalization of the sintered bed is necessary. After sintering, the octadecylated surface was renewed by treatment with a solution containing dimethyloctadecylchlorosilane.

Adam et al. [12] presented a method to prepare particle sintered monolithic columns in a single step by a hydrothermal treatment using water for the immobilization process. By carefully controlling the immobilization temperature and other parameters, the column can be prepared without damage to the surface of the reverse-phase silica, and thereby in can be used directly for separation after sintering.

Another possibility for the stabilization of packings and thus eliminating the need for frits is the embedding of packed particles in a rigid matrix. Particle-entrapped monolithic columns were prepared by introducing the entrapping solution after the column had been packed. The method developed by Chirica and Remcho [13] makes use of silicate sol solutions to fill the packed capillaries with subsequent heating. Both silica-based reverse-phase packing material and molecular imprinted polymeric packing were entrapped by silicate. The reported efficiencies of these columns are similar to that of a packed column. Some authors proposed another immobilization design that involved the entrapment of a conventional packed bed in an organic-based matrix [14]. This approach involves in-situ polymerization of a monomeric mixture that generates a solid porous polymer in which individual components and/or subsequent derivatization dictate the retention mechanism.

Dulay et al. [15] reported the preparation of particle-loaded continuous-bed columns in which ODS particles were loaded in a sol-gel matrix that was subsequently

covalently bonded to the capillary inner wall. The sol-gel network was integrally fixed to the walls of the capillary through covalent bonding of the silanol groups between the sol-gel matrix and the capillary wall. In contrast to a pure sol-gel monolith, the particle-loaded monolith did not display obvious shrinkage because the ODS particles helped to decrease the stress within the matrix. However, cracks around the ODS particles were noticed, possibly because of phase separation between hydrophobic ODS surface and the hydrophilic sol-gel matrix.

1.4.5. Polymeric monolithic columns

Historically, Kubin et al. were most likely the first who published the preparation of a continuous polymer matrix for chromatography while attempting to replace natural polysaccharide gel beads with a highly swollen poly(2-hydroxyethyl methacrylate) gel for the low pressure size-exclusion chromatography of proteins [16]. However, the permeability of this continuous bed gel was far too low to make the material useful. The first operating monolithic columns were prepared from open-pore polyurethane foams in the early 1970s and used as stationary phases for both liquid and gas chromatography. These materials were found to suffer from excessive swelling and softening in some solvents [17-19].

A real explosion of interesting monolithic materials as chromatographic sorbents followed the renewed interest in capillary electrochromatography in the

second half of the 1990s. A wide variety of monolithic approaches has been developed and successfully applied for efficient separations in the CEC mode.

Both organic and inorganic polymer-based monoliths have been prepared.

The preparation of monolithic porous polymer rods is a simple and straightforward process. A simplified scheme of this process is shown in **Figure 1.6.**

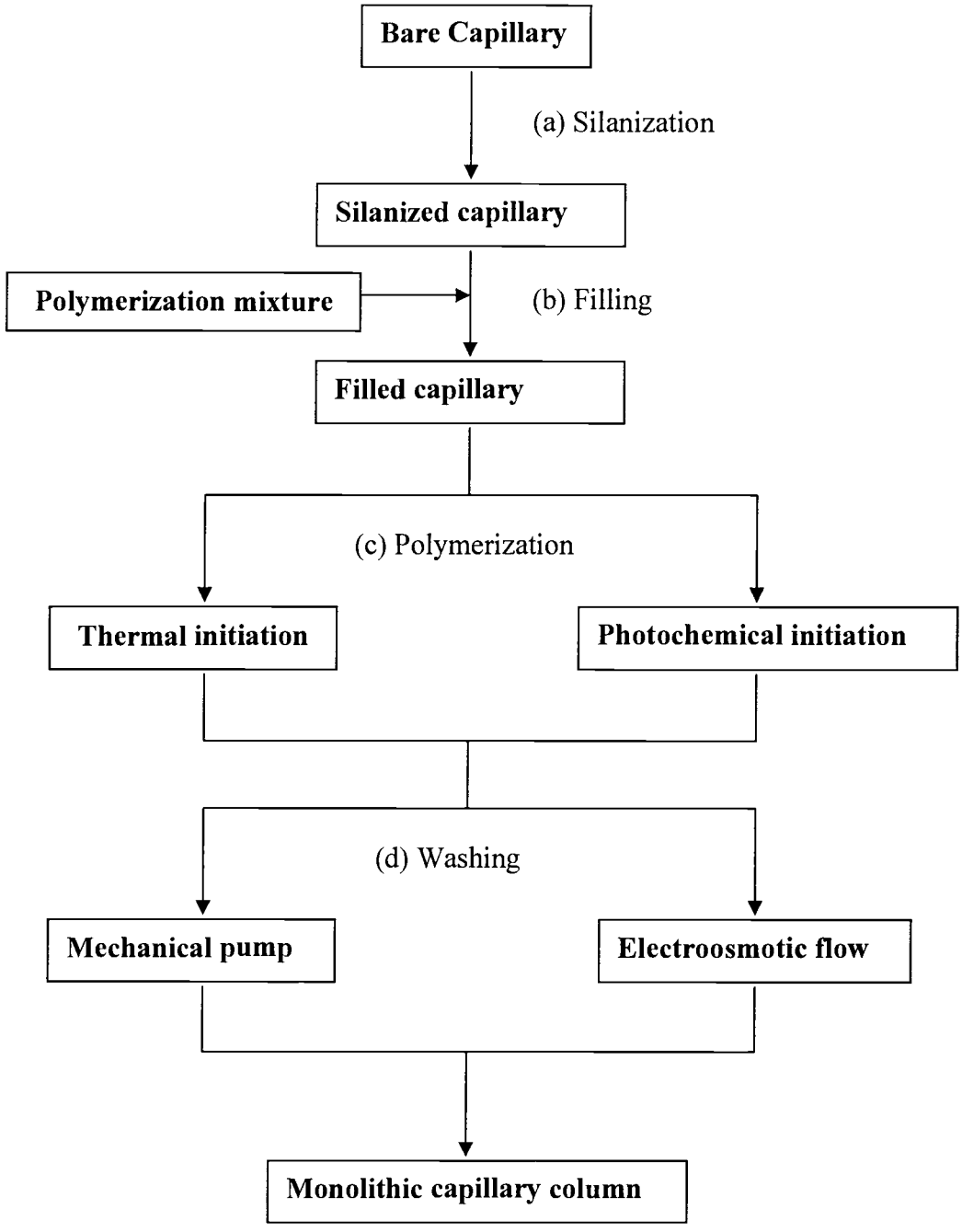

Figure 1.6. Preparation of a monolithic column. (a) silanization of the inner wall of the column allows chemical attachment of the polymer, (b) the capillary is filled with a mixture of liquid precursors (polymerization mixture), (c) polymerization is initiated by temperature or UV radiation, (d) removal of the unreacted components. According to ref. [20].

The mold, typically a segment of capillary tubing or a channel in a microchip, is filled with the polymerization mixture consisting of the monomers, initiator, and porogen solvent. The polymerization is then triggered by heating or by UV irradiation. Once polymerization is completed, the monolith is flushed with a solvent to remove the porogens and any other soluble compounds that might remain in the polymer.

Chemical attachment of polymer to the inner wall of the column is necessary in order to prevent the movement of monolith during the wash and separation procedure. Silanization of the inner wall of the capillary is similar in process to preparation of a coated capillary for capillary zone electrophoresis [21]. The capillary is washed with a strongly basic solution so that the siloxane groups at the inner surface are hydrolyzed, thereby increasing the density of silanol groups serving as anchors for the subsequent silanization. Then the capillary column is filled with a bifunctional reagent solution, typically γ-(trimethoxysilyl)propyl methacrylate in solution, and allowed to react for a period of time. After such a treatment, Si-O-Si-C bonds are formed between the capillary wall and the reactive methacryloyl groups, which are available for subsequent attachment of the monolith to the wall during the polymerization reaction.

The large number of monomers that may be used directly in the preparation of polymer monoliths allows for virtually unlimited choices of surface chemistry. Some of the reagents that have been used for the preparation of porous monoliths are shown in **Figure 1.7.** These monomers incorporate a wide selection of functionalities varying from very hydrophilic (acrylamide, 2-acrylamido-2-methyl-1-propanesulfonic acid) to hydrophobic (styrene, butylmethacrylate).

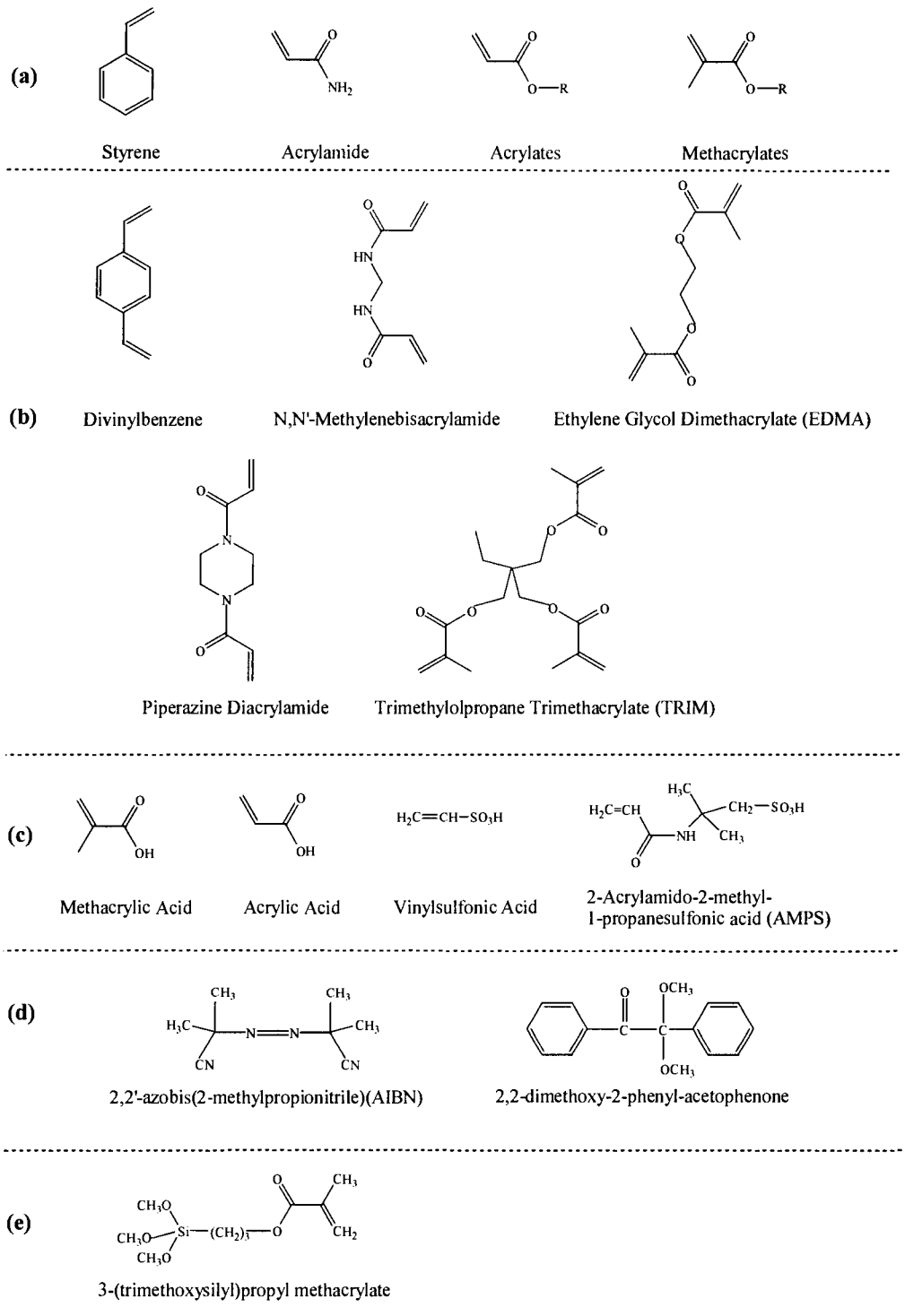

Figure 1.7. Reagents used for the preparation of polymer monolithic columns. (a) monomers with functional groups, (b) crosslinking reagents, (c) charged monomers responsible for the electroosmotic flow generation, (d) initiators, (e) silanization reagent.

So far, the monoliths based on polyacrylamides, polystyrenes and polymethacrylates are the most commonly reported.

1.4.5.1. Acrylamide-based monoliths

Acrylamide-based monoliths can be synthesized either in aqueous solution [21-27] or organic solvents [28-32]. Hjerten et al first reported the preparation of continuous CEC beds involving highly crosslinked acrylamide polymers in 1995 [21]. This original approach was tedious including two individual polymerizations and a chemical functionalization of the matrix.

The same group subsequently developed a much simpler procedure [22]. A polymerization mixture consisting of an aqueous solution of acrylamide, piperazine diacrylamide, and vinylsulfonic acid with added stearyl methacrylate and butyl methacrylate to control the hydrophobicity of the gel was sonicated with a surfactant to form an emulsion of the hydrophobic monomer in the aqueous solution. The mixture was immediately drawn into a capillary, where the polymerization was completed. The presence of the strongly acidic sulfonic acid functionalities afforded EOF that remained constant over a broad pH range.

The process of sonication used for dispersion of water-insoluble monomers can be avoided if the proper solvent is used to dissolve all reagents (hydrophobic and hydrophilic). Palm and Novotny [28] used mixtures of aqueous buffer with N-methylformamide to obtain homogeneous polymerization solutions consisting of

acrylamide, acrylic acid, methylene bisacrylamide, and alkyl acrylates (C4, C6, and C12). The composition of the mixed buffer/ N-methylformamide solvent depended on the type of alkyl acrylate used, and varied from 50/50 for butyl acrylate to 5/95 for dodecyl acrylate.

1.4.5.2. Polystyrene-based monoliths

The preparation of polystyrene-based monoliths was first reported by Horvath et al. in 1999 [10]. They demonstrated the syntheses of rigid monoliths using mixtures of chloromethylstyrene and divinylbenzene in the presence of various porogenic solvents such as methanol, ethanol, propanol, toluene, and formamide. The charged functional groups were introduced by reaction of surface chloromethyl groups with *N,N*-dimethyloctylamine. There capillary columns possessing positively charged surface functionalities were then used for the reversed-phase separation of basic and acidic peptides.

Xiong et al. also reported the preparation of monolithic columns by polymerization of styrene and divinylbenzene in the presence of toluene as the porogenic solvent [33].

1.4.5.3. Methacrylate-based monoliths

Extensive studies on methacrylate-based monoliths were presented by Svec and co-workers [34-41]. The methacrylate monolithic columns have been synthesized using R-methacrylate (R is a functional group, for example: butyl, glycidyl, lauryl, octadecyl, etc.), ethylene glycol dimethacrylate as crosslinker, and 2-acrylamido-2-methyl-1-propanesulfonic acid (AMPS). Usually the polymerization takes place in the presence of a ternary porogen consisting of 1-propanol, 1,4-butandiol and water. Monolithic columns prepared using this porogen system possessed efficiencies of over 210000 plates/m for the separation of a model mixture of aromatic compounds [41].

Many other groups have also prepared and studied methacrylate-based monoliths [42-50]. For example, Jiang et al. described the effect of varying the porous properties of methacrylate-based monolithic columns on the separation of different analytes [42]. The columns were characterized by mercury intrusion porosimetry, SEM and nitrogen absorption/desorption. For small alkyl benzene analytes, the separation efficiency improves as the size of the macropores decreases. However, in the case of bulkier analytes such as multi-substituted benzenes, higher separation efficiencies were observed with monoliths possessing very large pore sizes. Their findings demonstrate the importance of tailoring the porous structure to best fit a specific type of analysis.

The inorganic porous polymer columns, typically silica-based monolithic columns, are prepared using a sol-gel process. The procedure is similar to that used in the preparation of organic monolithic columns. The pretreatment of the silica capillary is also necessary to facilitate the attachment of the silica matrix to the wall. After pretreatment of the capillary with sodium hydroxide [51], hydrochloric acid [52] or water [53] at a relatively high temperature, sol-gel solution is introduced into the capillary column, and a three-dimensional network is created when hydrolysis and polycondensation reactions of the solution are completed. The prepared porous monolithic matrix could be then derivatized to a reversed-phased by on column reaction with silane reagent. For example, Tanaka and co-workers [51, 54] reported the preparation of a macroporous silica gel network by in situ hydrolysis and polymerization of tetramethoxysilane and poly(ethylene oxide). The silica monolith formed was then reacted with octadecyldimethyl-N,N-diethylaminosilane to form a reversed-phase chromatographic surface.

A drawback of the direct polymerization approach is that the polymerization conditions optimized for one polymerization system cannot be transferred directly to another without further experimentation. Therefore, the use of new monomer mixtures always requires optimization of polymerization conditions in order to achieve the desired properties of the resulting monolith.

The preparation of monolithic columns in CEC has gained significant interest. Today, some commercial products have become available. Although monolithic columns are unlikely to replace particulate supports, they can serve as an effective

complementary option. The fact that monolithic materials can easily be prepared even within very narrow channels by a single in situ polymerization step and their formation restricted to a specific area using UV-initiated polymerization through a suitable mask, makes them perfect candidates for application in miniaturized analytical systems on-chip.

References:

1. Pretorius, V.; Hopkins, B.; Schieke, J. *J.Chromatogr.*, **1974**, *99*, 23.

2. Jorgenson, J.W.; Lukacs, K.D. *J.Chromatogr.*, **1981**, *218*, 209.

3. Knox, J.H.; Grant, I.H. *Chromatographia*, **1987**, *24*, 135.

4. Remcho, V.T. *Chem Educator*, **1997**, 2.

5. Mysels, K. *Intoduction to Colloid Chemistry*; Interscience: New York, **1959**.

6. Shaw, D.J. *Electrophoresis*, Academic Press, London, **1969**.

7. Tan, J. Z.; Remcho, V.T. *Anal. Chem.*, **1997**, *69*, 581.

8. Tan, J. Z.; Remcho, V.T. *Electrophoresis*, **1998**, *19*, 2055.

9. Pesek, J.J.; Matyska, M.T. *J. Chromatogr. A*, **2000**, *887*, 31.

10. Gusev, I.; Huang, X.; Horvath, C. *J. Chromatogr. A*, **1999**, *855*, 273.

11. Asiaie, R.; Huang, X.; Farnan, D.; Horvath, C. *J. Chromatogr. A*, **1998**, *806*, 251.

12. Adam, T.; Unger, K.K.; Dittmann, M.M.; Rozing, G.P. *J. Chromatogr. A,* **2000**, *887*, 251.

13. Chirica, G.S.; Remcho, V.T. *Electrophoresis*, **1999**, *20*, 50.

14. Chirica, G.S.; Remcho, V.T. *Anal. Chem.,* **2000**, *72*, 3605.

15. Dulay, M.T.; Kulkarni, R.P.; Zare, R.N. *Anal. Chem.,* **1998**, *70*, 5103.

16. Kubin, M.; Spacek, R.; Chromecek, R. *Collect. Czech. Chem. Commun.* **1967**, *32*, 3881.

17. Ross, W.D.; Jefferson, R.T. *J. Chromatogr. Sci.* **1970**, *8*, 386.

18. Schnecks, H.; Bieber, O. *Chromatographia* **1971**, *4*, 109.

19. Hileman, F.D.; Sievers, R.E.; Hess, G.G.; Ross, W.D. *Anal. Chem.* **1973**, *45*, 1126.

20. Svec, F.; Peters, E.C.; Sykora, D.; Yu, C., Frechet, J.M.J. *J. High Resol. Chromatogr.* **2000**, *23*, 3.

21. Hjerten, S; Eaker, D.; Elenbring, K.; Ericson, C.; Kubo, K.; Liao, J.-L.; Zeng, C.-M.; Lidstrom, P.-A.; Lindh, C.; Palm, A.; Srichiayo, T.; Valtcheva, L.; Zhang, R. Jpn. J. *Electrophoresis* **1995**, *39*, 105.

22. Liao, J.L.; Chen, N.; Ericson, C.; Hjerten, S. *Anal. Chem.,* **1996**, *68*, 33468.

23. Ericson, C.; Liao, J.L.; Nakazato, K.; Hjerten, S. *J. Chromatogr. A* **1997**, *767*, 33.

24. Ericson, C.; Hjerten, S. *Anal. Chem.,* **1999**, *71*, 1621.

25. Hoegger, D.; Freitag. R. *J. Chromatogr. A* **2001**, *914*, 211.

26. Hoegger, D.; Freitag. R. *J. Chromatogr. A* **2003**, *1004*, 195.

27. Hoegger, D.; Freitag. R. *Electrophoresis* **2003**, *24*, 2958.

28. Palm, A.; Novotny, M.V. *Anal. Chem.,* **1997**, *69*, 4499.

29. Starkey, J.A.; Mechref. Y.; Byun, C.K.; Steinmetz, R.; Fuqua, J.S.; Pescovitz, O.H.; Novotny, M.V. *Anal. Chem.,* **2002**, *74*, 5998.

30. Que, A.H.; Novotny, M.V. *Anal. Bioanal Chem.,* **2003**, *375*, 599.

31. Righetti, P.G. *J. Chromatogr. A* **1995**, *698*, 3.

32. Zhang, M.Q.; Rassi, Z. El. *Electrophoresis* **2001**, *22*, 2593.

33. Xiong, B.H.; Zhang, L.H.; Zhang, Y.K.; Zou, H.F., Wang, J.D. *J. High Resolut. Chromatogr.* **2000**, *23*, 67.

34. Svec, F.; Frechet, J.M.J. *Anal. Chem.,* **1992**, *64*, 820.

35. Viklund, C.; Svec, F.; Frechet, J.M.J.; Irgum, K. *Chem. Mater.* **1996**, *8*, 744.

36. Petro, M.; Svec, F.; Gitsov, I.; Frechet, J.M.J. *Anal. Chem.* **1996**, *68*, 315.

37. Peters, E.C.; Petro, M.; Svec, F.; Frechet, J.M.J. *Anal. Chem.* **1997**, *69*, 3646.

38. Peters, E.C.; Petro, M.; Svec, F.; Frechet, J.M.J. *Anal. Chem.* **1998**, *70*, 2288.

39. Peters, E.C.; Petro, M.; Svec, F.; Frechet, J.M.J. *Anal. Chem.* **1998**, *70*, 2296.

40. Yu, C.; Svec, F.; Frechet, J.M.J. *Electrophoresis* **2000**, *21*, 120.

41. Svec, F.; Peters, E.C.; Sykora, D.; Frechet, J.M.J. *J. Chromatogr. A* **2000**, *887*, 3.

42. Jiang, T.; Jiskra, J.; Claessens, H.A.; Cramers, C.A. *J. Chromatogr. A* **2001**, *923*, 215.

43. Wu, R.; Zou, H.F.; Ye, M.L.; Lei, Z.D.; Ni, J.Y. *Anal. Chem.* **2001**, *73*, 4918.

44. Zhang, L.I.; Ping, G.; Zhang, L.; Zhang, W.; Zhang, Y. *J. Sep. Sci.* **2003**, *26*, 331.

45. Ping, G.; Zhang, W.; Zhang, L.; Zhang, L.; Shan, Y.; Zhang, Y.; Schmitt-Kopplin, P.; Kettrup, A. *Chromatographia* **2003**, *58*, 803.

46. Ping, G.C.; Zhang, W.B.; Zhang, L.; Zhang, L.H.; Schmitt-Kopplin, P.; Kettrup, A.; Zhang, K. *Chromatographia* **2003**, *57*, 777.

47. Ping, G.C.; Zhang, W.B.; Zhang, L.H.; Schmitt-Kopplin, P.; Zhang, Y.K.; Kettrup, A *Chromatographia* **2003**, *57*, 629.

48. Ping, G.C.; Zhang, Y.K.; Zhang, W.B.; Zhang, L.; Zhang, L.H.; Schmitt-Kopplin, P.; Kettrup, A.; Zhang, K. *Electrophoresis* **2004**, *25*, 421.

49. Bandilla, D.; Skinner, C.D. *J. Chromatogr. A* **2003**, *1004*, 167.

50. Doneanu, A.; Chirica, G.C.; Remcho, V.T. *J. Sep. Sci.* **2002**, *25*, 1252.

51. Ishizuka, N.; Minakuchi, H.; Nakanishi, K.; Soga, N., Nagayama, H.; Hosoya, K.; Tanaka, N. *Anal. Chem.* **2000**, *72*, 1275.

52. Fujimoto, C. *J. High Resolut. Chromatogr.* **2000**, *23*, 89.

53. Hayes, J.D.; Malik, A. *Anal. Chem.* **2000**, *72*, 4090.

54. Tanaka, N.; Nagayama, H.; Kobayashi, H.; Ikegami, T.; Hosoya, K.; Ishizuka, N.; Minakuchi, H.; Nakanishi, K.; Cabrera, K.; Lubda, D. *J. High Resolut. Chromatogr.* **2000**, *23*, 111.

CHAPTER 2

MICROFLUIDIC DEVICES

Many disciplines of science and technology have converged in the last few years to create exciting challenges and opportunities that involve a new generation of integrated microfabricated devices. The development of these devices involves both established and evolving technologies, including microlithography, micromachining, microelectromechanical systems (MEMS technology), microfluidics and nanotechnology.

Early on, the electronics industry realized that miniaturization in the form of the silicon microchip represented an elegant solution to the problem of complexity, and this industry has successfully exploited miniaturization to reduce the size of devices while increasing their capacity and functionality. The value in applying this same concept to the analytical sector, in particular in the field of separations, has been known for some time. One of the earliest attempts to miniaturized analytical tools came from Terry and colleagues. They constructed a gas chromatograph (GC) on the surface of a 2-inch silicon wafer that was then bonded to a glass plate [1].

While the enhanced analytical capabilities of microfabricated chip technology for expediting electrophoretic separations has been established [2-8], the true power of this technology lies in the potential to miniaturize and integrate existing technologies in a manner that allows for sample preparation and analysis to be seamlessly carried out on a single device.

2.1. Materials for microchip fabrication

Most of the microfluidic systems are fabricated in glass and silicon by technologies derived from microelectronics. Glass substrates are the most common because of their good optical properties, well-understood surface chemistry and highly developed microfabrication methods.

Since the early work in the field of microfluidics, there has been a rapid expansion into new types of materials, especially polymers. In contrast to silicon and glass, polymers are inexpensive and provide an opportunity for mass production of microfluidic devices. A wide range of polymer materials has been used for microfabrication processes including: polyamide (PA), polyethylene (PE), polypropylene (PP), polystyrene (PS), polymethylmethacrylate (PMMA), cyclic olefin copolymers (COC), polycarbonate (PC) and polydimethylsiloxane (PDMS).

The following sections describe typical fabrication procedures for both glass and polymer microchips.

2.2. Fabrication of Glass Microchips

The use of glass in μTAS applications is prompted by its unique properties. Glass is resistant to many chemicals, optically transparent and dielectric (and can therefore withstand the high voltages used in electrokinetically driven separations). Other advantages of glass are its high thermal stability and relative biocompatibility.

The microfabrication process in glass is well understood, easily implemented, and to a certain extent versatile. In addition, the chemistries originally developed for fused-silica capillaries used in capillary electrophoresis are directly applicable to glass substrates.

Features in glass substrates are usually generated using standard photolithographic technologies [9-12]. **Figure 2.1.** presents a diagram of such a procedure. First a thin film of metal is deposited onto the entire surface of the wafer followed by coating with a photoresist. The metallic layer serves to improve the adhesion of the photoresist to the substrate wafer during the etching process. The photoresist is exposed to UV radiation through a reusable photomask containing the desired channel layout. The photoresist and metal in the feature areas are removed, and the wafer etched to produce structures in the wafer. Wet etching of glass is mostly done with hydrofluoric acid (HF) or buffered hydrofluoric acid (BHF). The chemical reaction involved in wet etching glass is

$$SiO_2 + 4HF \longrightarrow SiF_4 + 2H_2O$$

(Because of the highly toxic nature of the HF used in glass etching, special safety precautions must be taken.)

Finally, the etched substrate is bonded to another piece of glass, into which reservoirs have been drilled, to form a finished microchip. The three most frequently

used glass-to-glass bonding methods are thermal fusion, anodic bonding, and adhesion bonding. Among these methods, fusion bonding has been the most popular.

Even though the mechanism of fusion bonding is not completely understood, it is believed to rely on a chemical reaction between hydroxide groups (OH-) present in the interface of the wafers:

$$\text{Si-OH} + \text{HO-Si} \longrightarrow \text{Si-O-Si} + H_2O$$

in which water is formed and released under heating, leading to the generation of covalent siloxane bonds (Si-O-Si).

However, while glass microchips continue to be employed successfully for many applications, they do have some disadvantages. First, a well-equipped cleanroom is required, and the use of hydrofluoric acid (HF) for etching the substrate requires special safety precautions. Secondly, glass is fragile and expensive and can often shatter during chip processing. Limitations in geometrical design due to the isotropicity of the etching process, which allows only shallow, mainly semicircular channel cross sections in glass substrates, are another disadvantage. Also, the procedure for glass-to-glass bonding is not always straightforward. It often takes several cycles before the glass is completely bonded in the area surrounding the reservoirs and the separation channel.

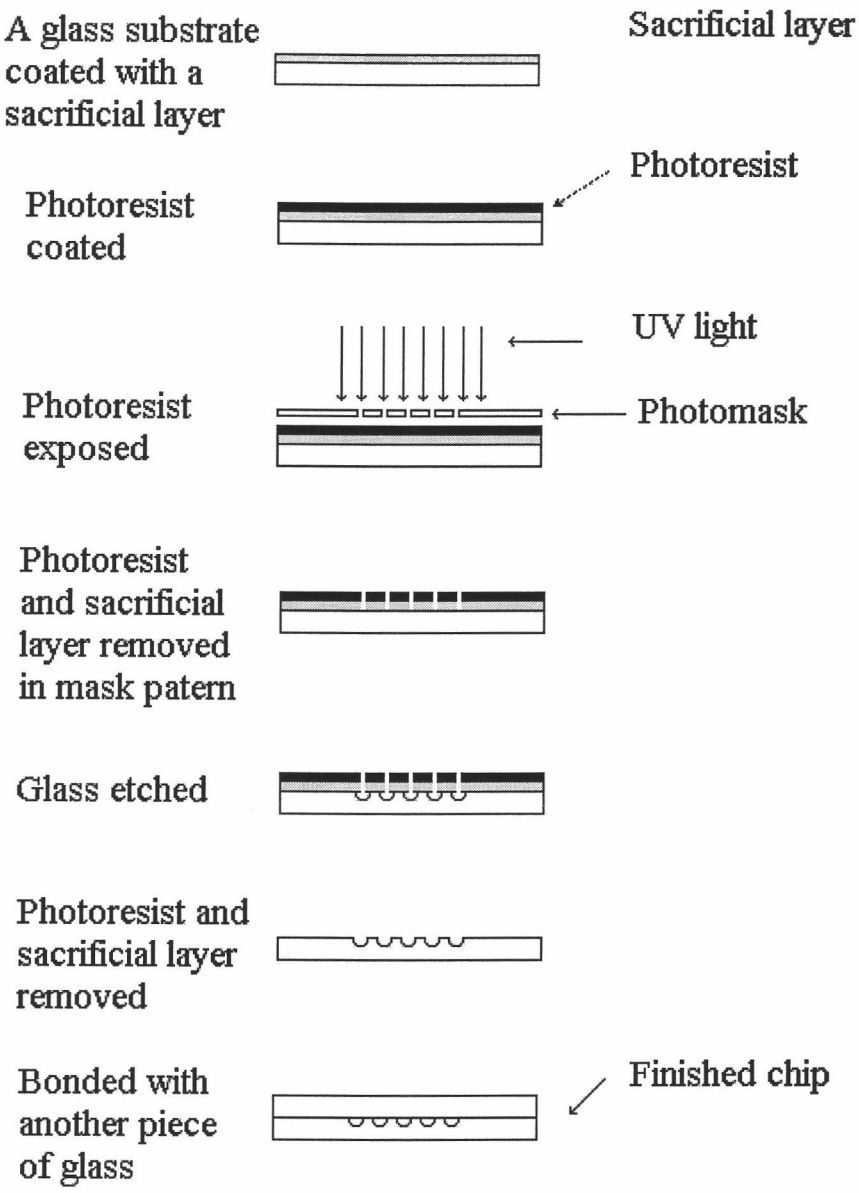

Figure 2.1. Photolithographic process for glass microchips

2.3. Fabrication of polymer microfluidic devices

As microfabrication methods and materials developed, new technologies that had not existed in the microelectronics world were introduced. In particular, the introduction of polymer microfabrication technologies has opened new possibilities for microfluidic applications. Polymers as substrate materials can avoid many of the above-mentioned glass microchips fabrication challenges. Their wide range of material properties, and their normally low-cost have attracted an enormous interest particularly as this opens up the road to the mass fabrication of disposable microfluidic devices.

A wide variety of polymer materials have been used for microfabrication processes. Some of the most intensely researched polymers are: polymethylmethacrylate (PMMA), polycarbonate (PC), poly(dimethylsiloxane) (PDMS) and poly(ethylene terephthalate) glycol (PETG).

The two major ways to micromachine polymers are replication from a master and direct machining. Replication methods, in which an inverse copy of a mold is produced, include injection molding, hot embossing, or casting.
Direct machining methods remove small amounts of polymer in places where microchannels or microwells, should be located. The material is removed either mechanically by a computer-controlled microdrill, or by means of radiation (intense UV or infrared radiation provided by a laser).

These methods are discussed in the following sections.

2.2.1. Injection molding

In the injection molding process [13], the polymer, in granular form, is melted and then injected into the cavity of a closed mold block, where the mold master is located. The molten plastic continues to flow into and fill the mold cavity until the plastic cools down to la highly viscous melt, and a cooled plastic part is ejected. In order to ensure good flow properties during the injection molding process, thermoplastics with low or medium viscosity are desirable. Cycle times of only 5-10 s are standard for most applications. Injection molding allows very high-throughput production with low cost.

2.2.2. Hot Embossing Process

One of the most widely used replication process to fabricate channel structures for microfluidic applications is hot embossing.

The hot embossing microfabrication process is itself a rather straightforward one [14-18]. The basic operating principle in the hot embossing process is to emboss the polymer substrate at a temperature above the glass transition temperature T_g of the polymer material and to de-emboss it when the polymer substrate temperature drops below T_g.

The replication master and the planar polymer substrate are mounted in the embossing system (**Figure 2.2.**). Both are heated separately in a vacuum chamber to a

temperature above T_g of the polymer material, which is typically of the order of 50-150 °C. The vacuum, although extending the overall cycle time, is necessary to prevent the formation of air bubbles due to entrapment of air in small cavities. In addition it prevents the nickel tool from corroding at elevated temperature, which extends the lifetime of the master. The master is brought into contact with the substrate and then embossed with controlled force. Typical embossing forces are of the order of 0.5-2 kN/cm^3. Still applying the embossing force, the master-substrate sandwich is then cooled to just below T_g. After reaching the lower cycle temperature, the embossing mold is detached from the substrate that now contains the desired features.

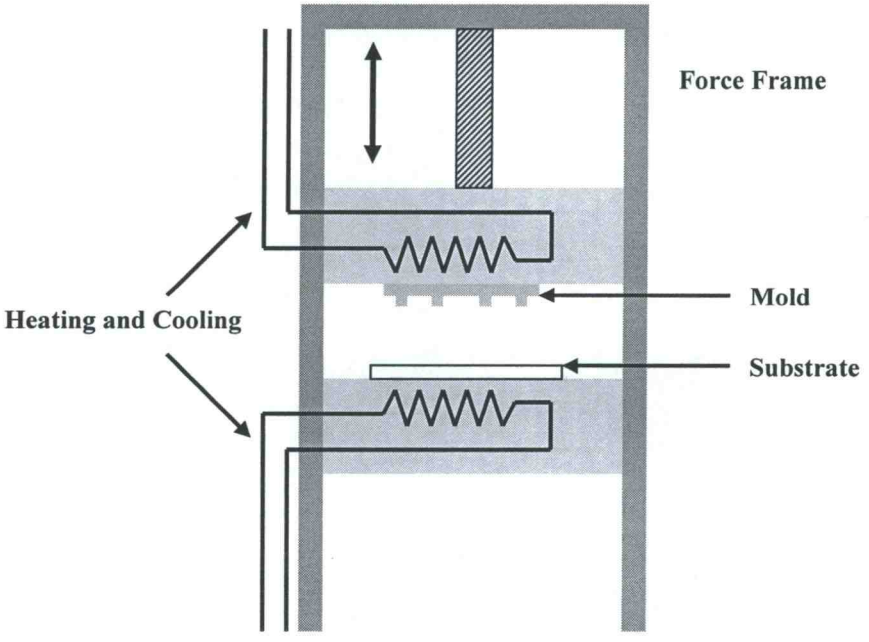

Figure 2.2. Schematic of a hot embossing machine.

2.2.3. Casting

Casting is a straightforward process that rapidly yields microstructures. Hot embossing and injection molding have in common that they use a heating and cooling cycle to soften and structure the polymer on a mold. Casting uses chemical processes to harden the polymer. Two components, a base and a hardener or cure, are mixed just prior to use. Immediately upon mixing, the chemical curing process starts and, after a certain amount of time, results in hardening of the polymer. The liquid mixture is poured into the mold and as the polymer sets it takes the shape of the mold. The polymer structure can then be removed from the mold.

Casting is often used in research laboratories for fast production of microchip prototypes [19-22].

2.2.4. Laser Ablation

The photoablation process involves absorption of a short-wavelength laser pulse to break covalent bonds in long-chain polymer molecules with production of a shock wave that ejects decomposed polymer fragments [23-25]. The laser energy can be specially patterned using a mask with the subsequent generation of microcavities and channels in various geometries or by controlling position of the laser with x-y stages. However, laser ablation does not lend itself to mass production.

2.2.5. Milling

Micromilling is a mechanical method that can be used to produce polymer microstructures. For micromilling, a small revolving cutting tool mechanically removes polymer material. A computer controls the position and movement of the cutting tool. The process is known as computer numerical control or CNC milling. Although CNC milling cannot achieve the very small feature sizes of the replication techniques it can produce structures with sizes down to 100 μm.

To create an enclosed channel usable for microfluidics, at the end of any of the above mentioned replication processes, a cover lid has to be put on top of the open channel. This can be realized with a number of technologies, depending on material and geometrical requirements. Some examples are: conformal sealing (for PDMS), use of adhesives, solvent bonding, thermal bonding, ultrasonic welding and laser welding.

2.3. Instrumentation and device operation

2.3.1. Microchip design

An attractive feature of a lab-on-a-chip device is the possibility of creating very complex structures that can be utilized for on-chip reactions, separations and detection. One can easily configure the chip design for a specific application.

The fundamental channel structure of most electrophoretic microdevices is a simple cross architecture, as illustrated in **Figure 2.3.** The cross consists of a long main separation channel, and three shorter side channels, which form the injector. The separation channel is several centimeters long. The three short side channels are only few millimeters in length, each terminating in a reservoir. All channels have depths of 20-50 μm and width of 60-100 μm.

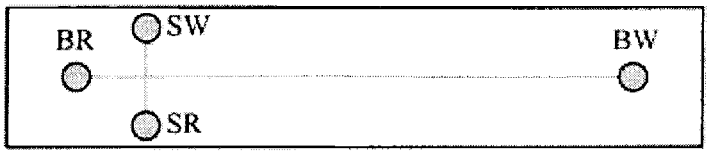

Figure 2.3. Schematic of the Micralyne microfluidic chip [26]

2.3.2. Injection

For many analytical techniques it is beneficial to be able to inject small, well-defined amounts of sample solutions. In microchip electrophoresis this can elegantly be performed as the size of the injection plug is defined by the size of the channel intersection and can further be manipulated by electric potential applied at the reservoirs.

There are two basic injection formats for microfluidic devices using electrokinetic flow: plug (or pinched) injection and gated injection. In pinched

injection, the sample is loaded from one side of a channel straight across by applying a potential drop. In addition, potentials are applied at the buffer inlet and outlet to prevent sample bleeding into the separation channel. In the following step, the sample is injected into the separation channel by switching the potentials accordingly (**Figure 2.4. a**). In this format a very narrow and well-defined plug is introduced.

A variation of the pinched injection is the double-T injection, where the two side channels are offset by a certain distance, and thereby increasing the volume to be injected.

In gated injection, the sample is continuously pumped around a corner and for injection the analyte flow is deflected into the separation channel by applying voltage through the intersection for a variable length of time (**Figure 2.4.b**).

Load position Inject & Run position

a) Plug injection

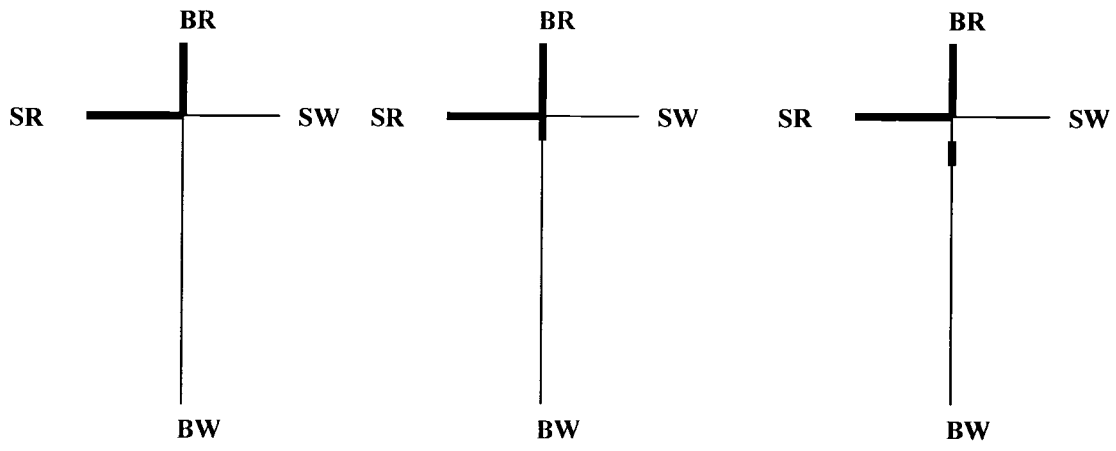

Load position Injection Run

b) Gated injection

Figure 2.4. Microfluidic injection schemes for introducing finite plugs of sample into channels. a) Plug (pinched) injection; b) Gated injection.

2.3.3. Detection

A drawback of injecting very narrow sample plugs is, however, that the detection sensitivity decreases with the decreasing amount of analyte injected. Development of appropriate detection methods providing sensitivity for a wide variety of analytes is accordingly a challenging task in microseparations.

Due to its high-sensitivity the most commonly used detection technique in microchip electrophoresis is laser-induced fluorescence (LIF) detection. Compared with other optical detection methods, this technique can be easily implemented in the experimental setup. A block diagram of the Micralyne (Alberta, Canada) Microfluidic Tool Kit instrument used in this work is shown in **Figure 2.5.** In brief, the kit consists of high-voltage power supplies coupled with a laser-induced fluorescence detection system. A detailed description of the instrumental setup used in this work is presented in Chapter 4.

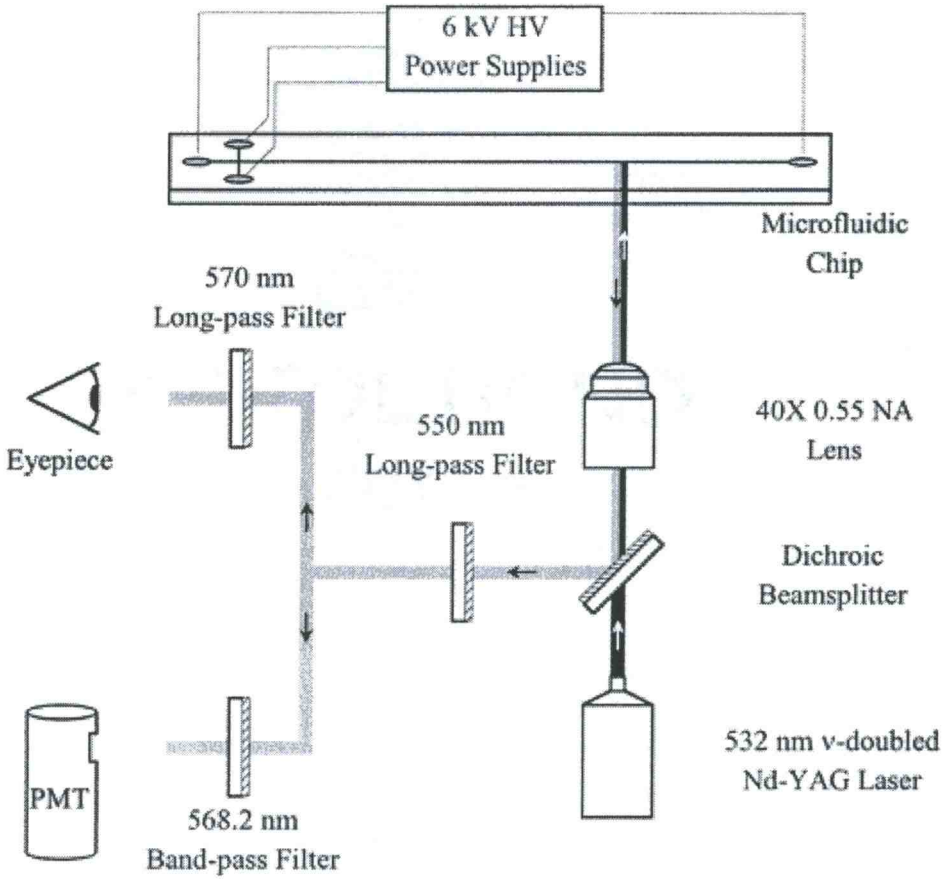

Figure 2.5. Schematic of the Micralyne (Alberta, Canada) Microfluidic Tool Kit [26]

At present, this exciting technology is under intensive research and development. It is anticipated that the use of polymer substrates in microfluidic systems will progress rapidly as the surface chemistries of various polymers are characterized, and as stable methods for surface modification of polymer microchannels are established. Chapter 5 describes some early work toward this goal.

References:

1. Terry, S.C.; Jerman, J.H., Angell, J.B. *IEEE Trans. Electron. Devices*, 1979, *26*, 1880.

2. Harrison, D.J.; Manz, A.; Fan, Z.; Luedi, H.; Widmer, H.M. *Anal. Chem.*, 1992, *64*, 1926.

3. Jacobson, S.C.; Ramsey, J.M. *Electrophoresis*, 1995, *16*, 481.

4. von Heeren, F.; Verpoorte, E.; Manz, A.; Thormann, W. *Anal. Chem.*, 1996, *68*, 2044.

5. Woolley, A.T., Lao, K.; Glazer, A.N.; Mathies, R.A. *Anal. Chem.*, 1998, *70*, 684.

6. Chiem N.H.; Harrison, D.J. *Electrophoresis*, 1998, *19*, 3040.

7. Munro, N.J.; Snow, K.; Kant, J.A.; Landers, J.P. *Clin. Chem.*, 1999, *45*, 1906.

8. Liu, S.; Shi, Y.; Ja, W.W.; Mathies, R.A. *Anal. Chem.*, 1999, *71*, 566.

9. Woolly, A.T.; Mathies, R.A. *Proc. Natl. Acad. Sci. USA*, 1994, *91*, 11348.

10. Fan, Z. H.; Harrison, D.J. *Anal. Chem.*, 1994, *66*, 177.

11. Jacobson, S.C.; Hergenroder, R.; Moore, A.W.; Ramsey, J.M. *Anal. Chem.*, 1994, *66*, 4127.

12. Koutny, L.B., Schmalzing, D.; Taylor, T.A.; Fuchs, M. *Anal. Chem.*, 1996, *68*, 18.

13. McCormick, R.M.; Nelson, R.J.; Alonso-Amigo, M.G.; Benvegnu, J.; Hoopwer, H.H. *Anal. Chem.*, 1997, *69*, 2626.

14. Martynova, L.; Locasico, L.E.; Gaitan, M.; Kramer, G.W.; Christensen, R.G.; MacCretan, W.A. *Anal. Chem.*, 1997, *69*, 4783.

15. Locasico, L.E.; Gaitan, M.; Hong, J.; Eldefrawi, M. *Proc. Micro-TAS '98*, Banff, Canada **1998**, 367.

16. Becker, H.; Dietz, W.; Dannberg, P. *Proc. Micro-TAS '98*, Banff, Canada **1998**, 253.

17. Becker, H.; Heim, U. *Sens. Actuators A*, **2000**, *83*, 130.

18. Heckele, M.; Bacher, W.; Muller, K.D. *Microsystem Technol.*, **1998**, *4*, 122.

19. Kim, E.; Xia, Y.; Whitesides, G.M. *Nature*, **1995**, *376*, 581.

20. Xia, Y.; Kim, E.; Zhao, X. M.; Rogers, J.A.; Prentiss, M.; Whitesides, G.M. *Science*, **1996**, *273*, 347.

21. Duffy, D.C.; McDonald, J.C.; Schueller, O.J.A.; Whitesides, G.M. *Anal. Chem.*, **1998**, *70*, 3451.

22. Anderson, J.R.; Chiu, D.T.; Jackman, R.J.; Cherniavskaya, O.; McDonald, J.C.; Wu, H.K.; Whitesides, S.H.; Whitesides, G.M. *Anal. Chem.*, **2000**, *72*, 3158.

23. Reyna, L.G.; Soberhart, J.R. *J. Appl. Phys.*, **1994**, *76*, 4367.

24. Roberts, M.A.; Rossier, J.S.; Bercier, P.; Girault, H. *Anal. Chem.*, **1997**, *69*, 2035.

25. Srinivasan, R.; Braren, B. *Chem. Rev.*, **1989**, *89*, 1303.

26. Crabtree, J.H.; Cheong, E.S.C.; Tilroe, D.A.; Backhouse, C.J. *Anal. Chem.*, **2001**, *73*, 4079.

CHAPTER 3

STARBURST DENDRIMERS AS MACROMOLECULAR PORE-TEMPLATES FOR STATIONARY PHASES IN CAPILLARY CHROMATOGRAPHY

Abstract

Methacrylate-based monolithic capillary columns for liquid chromatography and capillary electrochromatography were prepared within the confines of fused-silica tubing using Starburst (PAMAM) dendrimers to affect porosity. Different column porosities were obtained by varying the amount of the dendrimer template as evidenced by electron microscopy. Mercury intrusion porosimetry measurements provided additional information. The effect of dendrimer concentration on chromatographic performance was studied in detail.

3.1. Introduction

Capillary electrochromatography (CEC) is a rapidly growing area in analytical separations. In order for CEC to demonstrate its utility and promise as a chromatographic separation technique, significant advancements are needed in the area of column technology. Special interest has been shown towards developing new designs of capillary columns that do not require frits and thus are amenable to use in both fused silica capillaries and channels on microchips. Monolithic columns have recently been embraced as perhaps the most attractive alternative to conventional packed columns for liquid chromatography (LC) and CEC. A simple in situ polymerization process can be performed directly within the confines of a mold, typically a segment of capillary tubing or a channel on a microchip. Both silica [1-3] and organic [4-13] based monolithic columns have been synthesized. This procedure provides a sorbent for which frit formation and irreproducible packing are no longer issues.

The porosity of the polymeric stationary phase in monolithic columns is usually dictated by the nature and amount of the porogenic solvent employed. Aside from affecting porosity, adjustments of the amount and nature of the porogenic solvent(s), alter other properties such as the surface area, nature and swelling properties of the resulting monoliths. This can work to the advantage of the experiment, or to its disadvantage.

Recently, Chirica & Remcho [14] described a new synthetic method for preparation of monoliths with porosity dictated by the size of spherical silica particle templates. In addition to tailoring the pore size, this method offers the ability to influence the surface characteristics of the finished polymer by employing silica beads with specific surface chemistry.

In this study, we investigate new monolithic stationary phases that afford control over porosity and, to a certain degree, over the surface chemistry of the sorbent. The novelty of this study lies in the use of dendrimers for generation of uniform pore structures. Polyamidoamine (PAMAM) dendrimers (**Figure 3.1.**) represent an exciting class of macromolecules. Unlike classical polymers, dendrimers have a high degree of molecular uniformity, narrow molecular weight distribution, specific size and shape characteristics, and a highly-functionalized terminal surface. The PAMAM dendrimers are manufactured by a divergent repetitive growth technique and are typically based on an ethylenediamine (EDA) core with repeating tertiary amine/amide branching units.

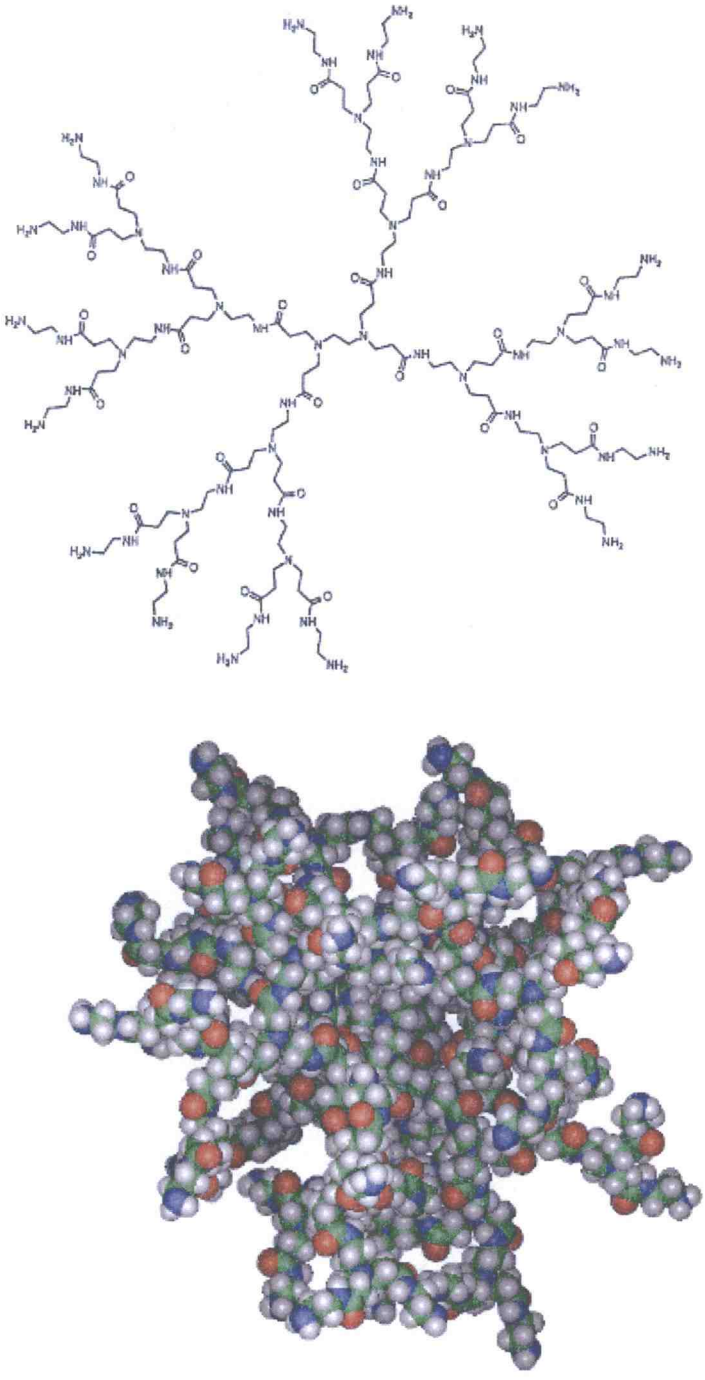

Figure 3.1. Structure of starburst dendrimers (generation 2.0), *illustrations from http://www.mmi.org/mmi/dendritech/index.html* (with permission).

A schematic of the preparation of monolithic columns with templated porosity is illustrated in **Figure 3.2.** The macromolecules are incorporated into a solution of functionalized monomers, cross-linker, solvent, and polymerization initiator. Thermal polymerization, followed by the removal of solvent and dendrimers, produces a continuous rod of polymer with uniform porosity and dendrimer-influenced surface character.

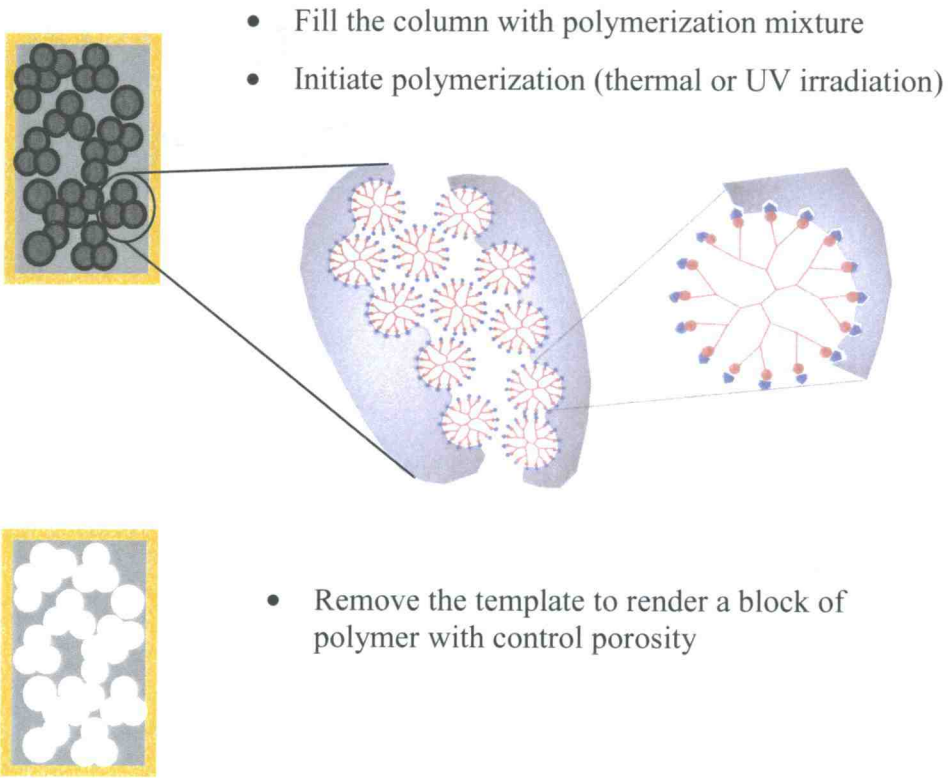

Figure 3.2. The general concept for preparation of monolithic columns with templated porosity.

3.2. Experimental Section

3.2.1. Chemicals and materials

Butyl methacrylate (BMA), ethylene dimethacrylate (EDMA), 2-acrylamido-2-methyl-propansulfonic acid (AMPS), 2,2'-azobisisobutyronitrile (AIBN), Starburst (PAMAM) dendrimer (generation 4.5; 10% solution in methanol), and [(methacryloxy)-propyl] trimethoxysilane were purchased from Aldrich (Milwaukee, WI, USA) and used as received. The solvents employed in the CE and CEC runs were HPLC grade and were purchased from Fisher Scientific (Pittsburgh, PA, USA). Fused silica tubing of 100 μm I.D.x 375 μm O.D. was purchased from Polymicro Technologies (Phoenix, AZ, USA).

3.2.2. Production of the lysozyme digest

Chicken egg lysozyme (Aldrich) was dissolved in 20 mM ammonium bicarbonate (pH 7.8) and digested using modified trypsin (Aldrich) (0.5 μg/mL) for ~ 72 h at 37°C.

3.2.3. Instrumentation

Electrochromatographic experiments were carried out using an Agilent/HP ^{3D}CE (Waldbronn, Germany) instrument, modified such that pressure of up to 12 bar can be applied on the inlet and/or outlet vials. Data acquisition and processing were performed with the Agilent ChemStation software. Samples were injected electrokinetically (5 kV for 3 sec). Pressure injection (50 mbar for 3 sec) was also used occasionally. The cassette temperature was set at 22 °C.

Examination of capillary columns during monolith preparation was achieved with a simple Stereomaster optical microscope (Fisher Scientific, Houston, TX, USA) with 40X magnification. The column morphology was studied using an AmRay (Bedford, MA, USA) scanning electron microscope (SEM) operated at 10 kV.

3.2.4. Column Preparation

3.2.4.1 Pretreatment of the capillary

For columns in which the monolith was anchored to the fused-silica capillary wall, functionalization of the walls was required. The fused-silica tubing was derivatized with [(methacryloxy)-propyl] trimethoxysilane, using a method developed by Hjertèn [15]. Briefly, the capillary was flushed with a solution of sodium hydroxide (1 M) followed by water for at least 30 minutes each. The capillary was filled with a

4:1000 (monomer/solvent; v/v) solution of [(methacryloxy)-propyl] trimethoxysilane and 6 mM acetic acid. The solution was kept in the capillary for at least 1 hour. The capillary was flushed with water for several minutes and finally emptied and dried with a flow of nitrogen.

3.2.4.2. Monolithic column preparation

AIBN (1 wt % with respect to the monomers) was dissolved in a monomer mixture consisting of 40% EDMA, 59.7% BMA and 0.3% AMPS. The solvent, methanol, was slowly admixed to the monomers in a 2:3 (v/v) ratio. Aliquots of 1 mL of this mixture were added to several vials containing specific amounts of Starburst (PAMAM) dendrimer. The dendrimer, commercially available as a 10% solution in methanol, was used after the removal of methanol by vacuum distillation. After addition of the monomer solution, the homogeneous mixtures were purged with nitrogen for 10 min. The capillary was filled with the polymerization mixture using a 100 μL syringe. Both ends of the capillary were sealed with rubber septa, and the column was submerged in a 60°C bath for 20 h. Using a syringe pump, the resulting monolith was washed with the mobile phase to flush out the residual reagents, dendrimers and methanol. With appropriate rinsing solutions, it is possible at this point to recover and reuse the dendrimer templates.

Using a small piece of PTFE tubing the monolithic column was joined to a fused-silica open tube onto which a detection window was burned.

In addition, selected polymers were prepared in "bulk" quantities. These polymers were ground and then washed with the mobile phase to remove the dendrimers and any residual reagents. After drying, the porosity of the polymers was determined by mercury intrusion porosimetry.

3.2. Results and Discussion

3.3.1. Physical characterization of the monoliths

For morphological characterization of the monolith, the polymer was sputter-coated with gold and examined with a scanning electron microscope. The SEM images presented in **Figure 3.3.** demonstrated that this procedure renders a highly permeable monolith with porosity dictated by the dendrimer concentration.

The structures of the various monolithic columns differ significantly, and depend on the dendrimer concentration in the polymerization mixtures. It is interesting to note that, at very high concentrations of dendrimer (400 μM), the microglobules become larger and the globule stacking and the channel distribution become less uniform. This is likely the causative factor behind the decrease in column efficiency and resolution achieved at the highest dendrimer concentrations studied.

High permeability of the polymeric monoliths is essential for their application as sorbents in extractions and chromatographic separations. Therefore the porosity of

the monolith is of great importance. In our study, different column porosities were obtained by varying the amount of the dendrimer template.

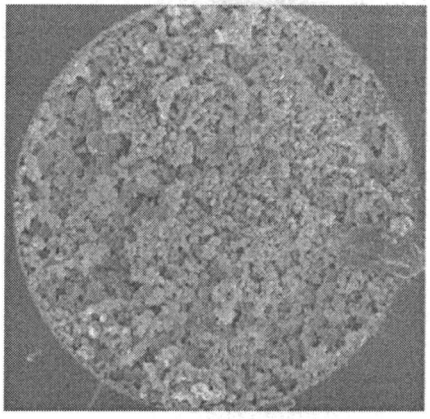

100 μM

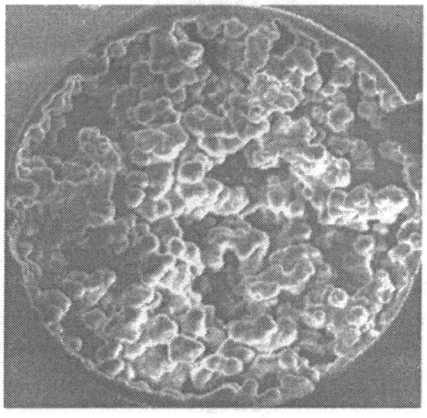

200 μM

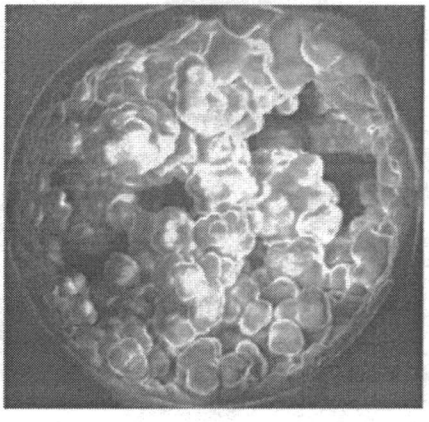

300 μM

Figure 3.3. SEM images of the monolithic columns prepared with different dendrimer concentrations.

The porosity data and the pore size distribution profiles of the monoliths in dried form were obtained by means of mercury intrusion porosimetry. These analyses were performed by Micromeritics Instrument Corporation (Norcross, GA) using a Micromeritics AutoPore mercury porosimeter.

Figure 3.4. shows the differential pore size distribution profiles for several porous polymers prepared using different dendrimer template concentrations. There is a noticeable difference between pore size distribution profiles for these columns. For instance, the mode pore diameter (the pore diameter at the maximum of the distribution curve) increases from 600 nm for column 1 (produced in the absence of dendrimers) to 700 nm for column 2 (50 μM dendrimers) and reaches 800 nm for column 3 (100 μM dendrimers). Based on these results, it appears that the average pore size of the monoliths can be adjusted to the desired one by carefully optimizing the dendrimer template concentration.

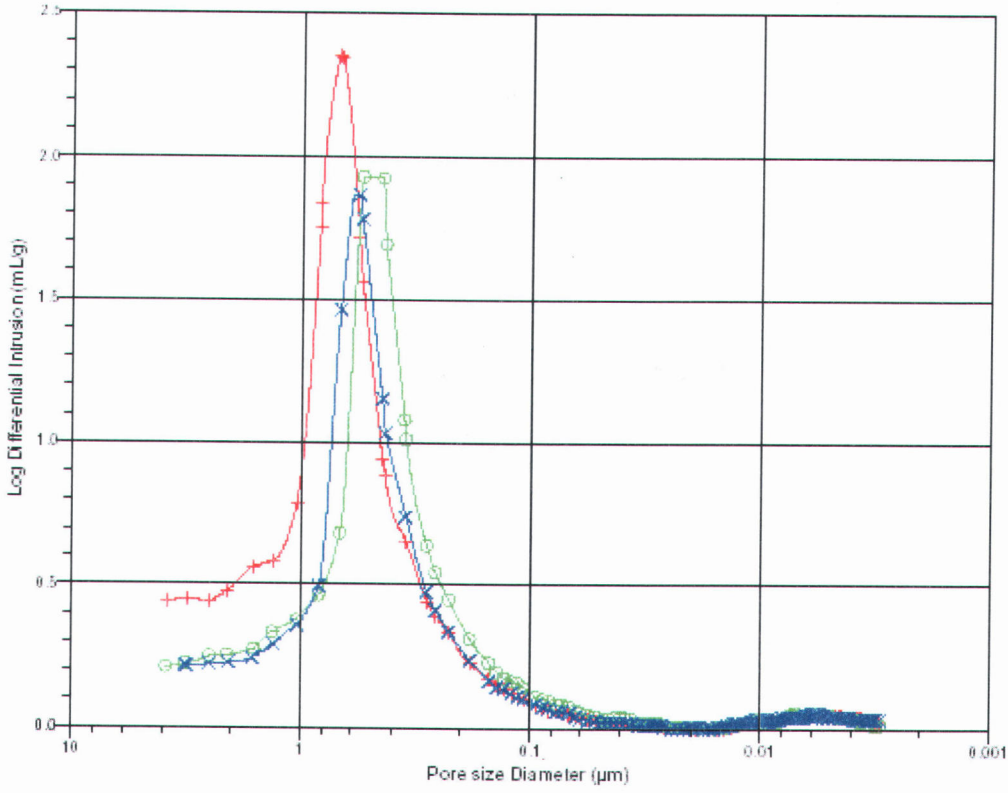

Figure 3.4. Differential pore size distribution profiles of porous polymers prepared using dendrimer template concentrations of 0 (o), 50 (x) and 100 (+) μM. All other monomer solution components as listed in the text.

3.3.2. Chromatographic characterization of the monolithic columns

The peak achievable efficiency of monolithic columns was examined in the CEC mode by measuring the peak width at half height for toluene in order to investigate the effect of dendrimer concentration on chromatographic performance. **Figure 3.5.** shows a plot of efficiency as a function of dendrimer template concentration. As dendrimer concentration increases from 0 to 400 μM, the column

efficiency increases from about 8,000 to 60,000 plates/m, reaching a maximum at 200 μM dendrimer concentration. As observed in the SEM data, at 400 μM dendrimer concentration, the pores become larger and less uniform, which is likely the cause of the decrease in column efficiency. The large size of the pores results in a smaller surface area and a larger total eluent volume; consequently the analyte is less retained and experiences greater diffusional relaxation, hence the lower efficiency.

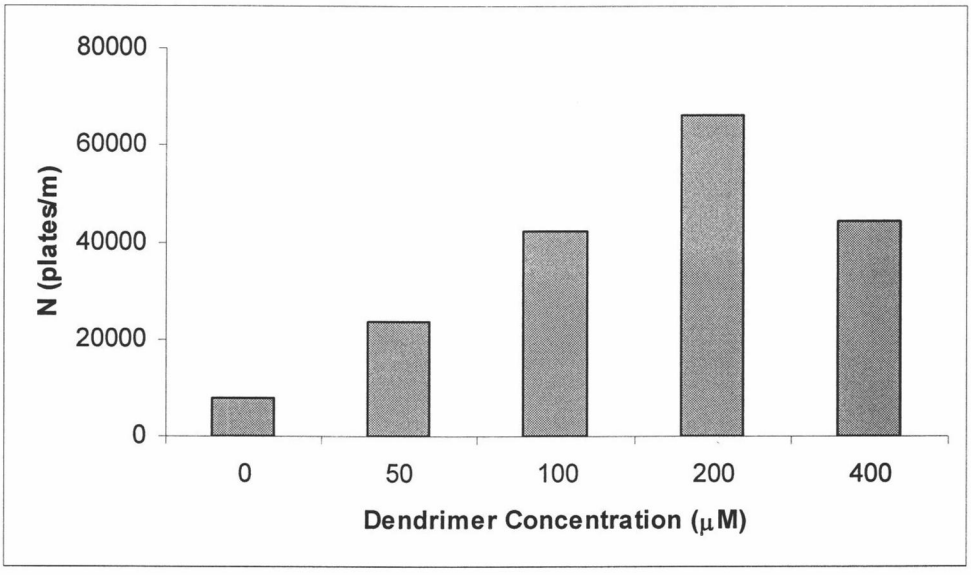

Figure 3.5. Variation of efficiency for toluene with dendrimer template concentration. Columns were prepared using the following polymerization mixture: EDMA 16%, total BMA and AMPS 24%, methanol 60%, AIBN 1 wt % (with respect to monomers) and dendrimer template concentrations of 0, 50, 100, 200 and 400 μM. Data were obtained by applying 20, 25 and 30 kV. Mobile phase: 80% acetonitrile: 20% phosphate buffer 5 mM (pH=7); UV detection at 254 nm.

Another parameter used to evaluate the chromatographic performance of these monolithic columns was resolution in the separation of acetone and toluene. As shown in **Figure 3.6.** and as anticipated, the dendrimer concentration had a similar effect on chromatographic resolution as on efficiency. The resolution increases with the dendrimer concentration and reaches a maximum at 200 μM dendrimer concentration. Again, a decrease in column performance was observed at 400 μM dendrimer concentration.

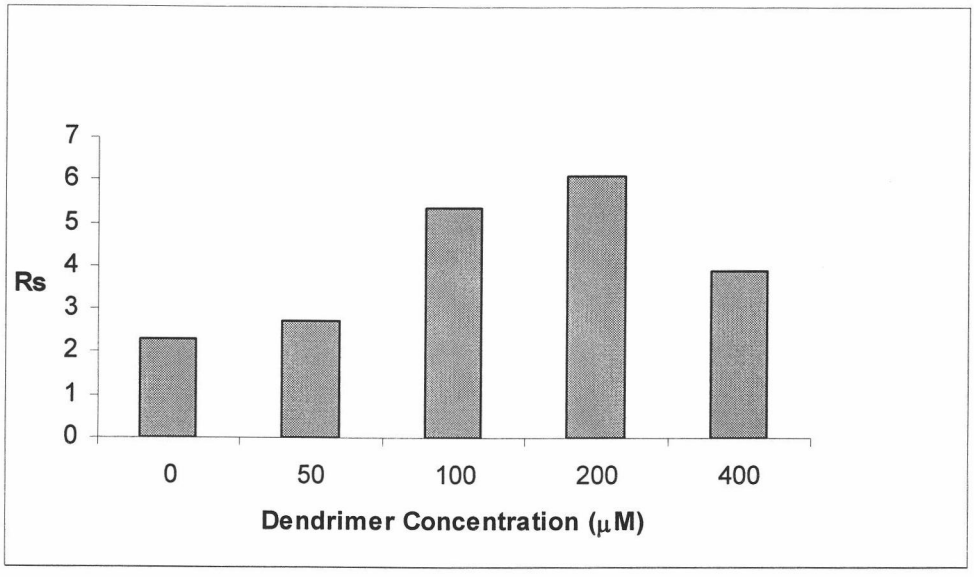

Figure 3.6. Variation in resolution of acetone and toluene with dendrimer concentration. Conditions as in Figure 4.

The performance of monolithic columns has mostly been evaluated using small, neutral organic molecules, which are typically separated under conditions of reverse-phase chromatography. To extend the range of monolithic column applications, the separation of lysozyme tryptic digest fragments was attempted on a column prepared using 50 μM dendrimer template. The chromatogram shown in **Figure 3.7.**, obtained using 40/60 ACN/40 mM phosphate buffer (pH=2) at an applied voltage of 10 kV, demonstrates the ability of these columns to separate complex mixtures.

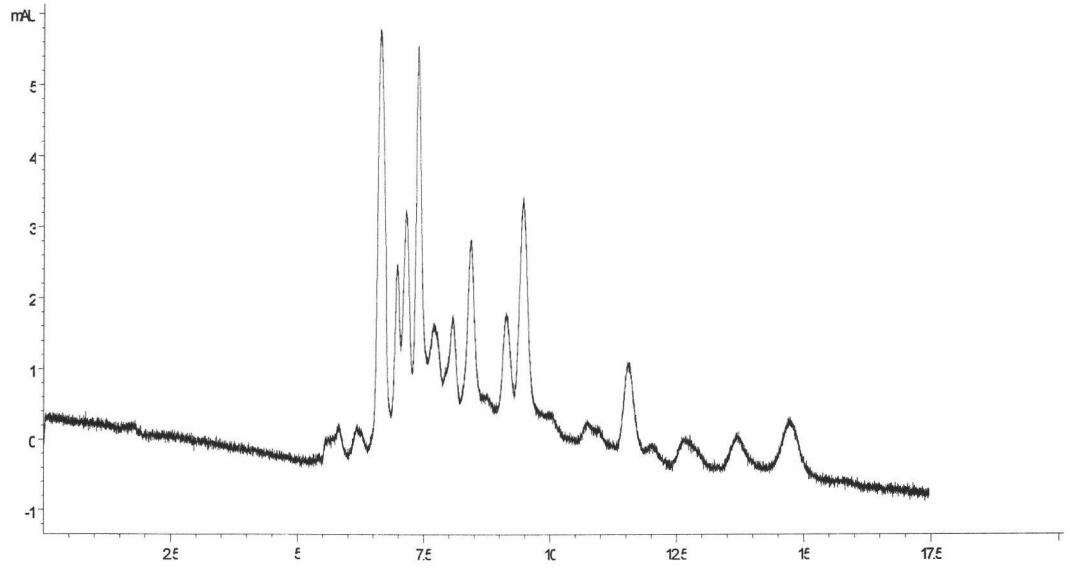

Figure 3.7. CEC separation of lysozyme tryptic digest fragments. Separation was performed on a 21 cm (L_{bed}), 31.5 cm (L_{tot}) column prepared using 50 μM dendrimer template. Buffer: 40% acetonitrile: 60% 40 mM phosphate buffer (pH=2). Applied voltage: 10 kV; UV detection at 200 nm.

3.2. Conclusion

A new class of porous polymer monoliths has been developed for use in capillary electrochromatography. While until recently the most popular means of controlling the porosity of monoliths has been by adjusting the amount and nature of the porogenic solvent or by incomplete polymerization, our approach, in which a macromolecular template (polyaminoamide (PAMAM) dendrimer) is used for pore generation offers a new alternative. Structural attributes of this template allowed for production of continuous polymeric rods exhibiting uniform porosity.

Reference:

1. Fields, S.M. *Anal. Chem.* 1996, *68*, 2709-2712.

2. Minakuchi, H., Nakanishi, K., Soga, N., Ishizuka, N., Tanaka, N. *Anal. Chem.* 1996, *68*, 3498-3501.

3. Minakuchi, H., Nakanishi, K., Soga, N., Ishizuka, N., Tanaka, N. *J. Chromatogr. A* 1997, *762*, 135-146.

4. Fujimoto, C. *Anal. Chem.* 1995, *67*, 2050-2053.

5. Liao, J-L., Chen, N., Ericson, C., Hjèrten, S. *Anal. Chem.* 1996, *68*, 3468-3472.

6. Palm, A., Novotny, M. *Anal. Chem.* 1997, *69*, 4499-4507.

7. Peters, E.C., Petro, M., Svec, F., Fréchet, J.M.J. *Anal. Chem.* 1997, *69*, 3646-3649.

8. Peters, E.C., Petro, M., Svec, F., Fréchet, J.M.J. *Anal. Chem.* 1998, *70*, 2288-2295.

9. Peters, E.C., Petro, M., Svec, F., Fréchet, J.M.J. *Anal. Chem.* 1998, *70*, 2296-2302.

10. Gusev, I., Huang, X., Horvath, Cs. *J. Chromatogr. A* 1999, *855*, 273-290.

11. Svec, F., Peters, E.C., Sýkora, D., Fréchet, J.M.J. *J. Chromatogr. A* **2000**, *887*, 3-29.

12. Svec, F., Peters, E. C., Sýkora, D., Yu, C., Fréchet, J.M.J., *J. High Resol. Chromatogr.* **2000**, *23*, 3-18.

13. Zou, H., Huang, X., Ye, M., Lou, Q. *J. Chromatogr. A* **2002**, *954*, 5-32.

14. Chirica, G.S., Remcho, V.T. *J. Chromatogr. A* **2001**, *924*, 223-232.

15. Hjertèn, S. *J.Chromatogr.* **1985**, *347*, 191-195.

CHAPTER 4

MICROCHIP ELECTROPHORESIS: PRINCIPLES AND APPLICATIONS

4.1. Introduction

Miniaturization of chemical analysis systems using microchips is an emerging technology. The concept of micro total-analysis systems (μTAS) introduced by Manz and coworkers in 1990 [1] triggered rapidly growing interest in development of microsystems in which all the stages if chemical analysis such as sample preparation, chemical reactions, analyte separation, analyte purification, analyte detection, and data analysis are performed in an integrated and automated fashion. The idea of lab-on-a-chip is basically to reduce chemical laboratories to a microscale system, hand-held size or smaller.

There are many advantages to using lab-on-a-chip over conventional chemical laboratories. One of the important advantages lies in its low cost. Many reagents and chemicals used in biological and chemical reactions are expensive, therefore the prospect of using very small amounts (micro- to nanoliter quantities) of reagents and chemicals for an application is very appealing. In addition, smaller amounts of reagents produce less waste and fewer harmful by-products. Another important advantage is the increased analysis speed that results from the small dimensions

associated with a chip [2]. Small size is also favorable to highly integrated parallel systems and portable monitoring devices.

As part of an interdisciplinary team with the objective to develop a nanomaterials synthesis microsystem, our group is involved in developing high-throughput nanoextraction technology for implementation in microsystems. The first step toward this objective was to evaluate the feasibility of transferring available separation techniques into microchip format.

Among the various separation techniques that could be integrated on microfluidic devices, capillary electrophoresis is the most promising [3-6]. There is no fundamental difference between microchip CE and conventional CE. The theory developed for capillaries is readily applicable to micromachined channels. The channel size on microchips (10-100 μm in width or depth) is similar to the size of fused-silica capillaries, but shorter lengths are obviously employed (1-10 cm).

The fundamental separation mechanism of capillary electrophoresis is based on differential electrophoretic mobilities of charged species when placed in an electric field. The motive force for bulk flow is electroosmosis. (A detailed description of electroosmotic flow is given in Chapter 1.) Electroosmosis, as a bulk driving force in microchips, has certain advantages, namely, absence of moving parts or valves, minimal backpressure effects and the possibility of controlling multiple channels with just a few electrodes.

This work reports on both fast and efficient separations of amino acids. In this initial study, glass was employed as a microchip substrate. Glass microchips are

optically transparent, enabling detection of the analytes by laser-induced fluorescence. In addition, the electroosmotic flow achieved in glass microchips is similar to that in fused-silica, making it easier to transfer separations from one format to another. An integrated sample injector allows electrokinetic injection of small sample volumes in a volume-defined injection scheme as described earlier.

4.2. Experimental Section

4.2.1. Reagents

Amino acids: glycine, L-histidine, and phenylalanine were obtained from Sigma-Aldrich (St. Louis, MO, USA). 5-carboxytetramethylrhodamine succinimidyl ester (5-TAMRA-SE) was purchased from Molecular Probes (Eugene, OR, USA). Sodium bicarbonate was purchased from Mallinckrodt Baker, Inc. (Paris, KN, USA). Sodium tetraborate decahydrate was obtained from Integra Chemical Company (Renton, WA, USA). Dimethylsulfoxide (DMSO) was purchased from EMD Chemicals, Inc. (Gibbstown, NJ, USA).

4.2.2. Microfluidic device

The microchips used in this work were manufactured at Micralyne Inc. (Edmonton, AB, Canada). A schematic of the microchip is shown in **Figure 4.1.**

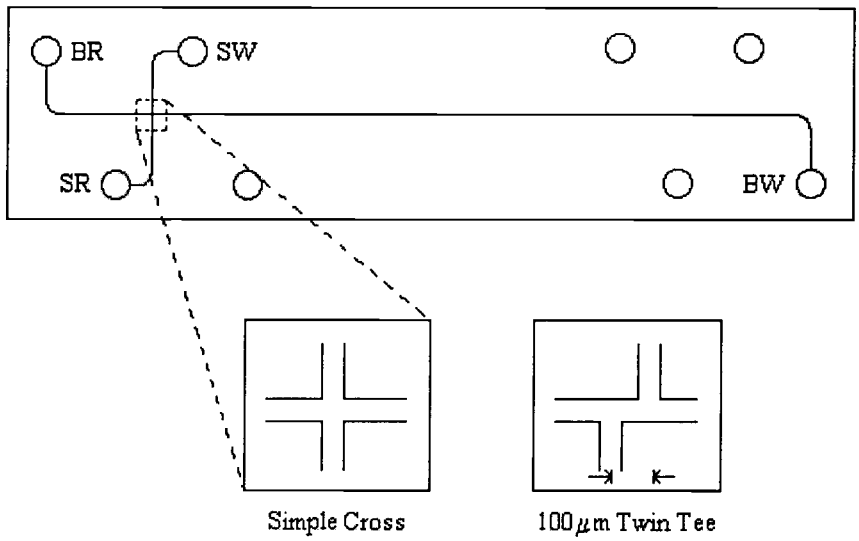

Figure 4.1. Schematic of a Micralyne standard microfluidic chip.

Each microchip device is 16 x 95 x 2.2 mm and made from 2 fused pieces of low fluorescence Schott Borofloat™ glass. Each plate is 1.1 mm thick with the bottom plate containing the etched pattern and the top plate containing the reservoir holes. The microchips consist of a cross-shaped intersection of an injection channel (9.64 mm) and a separation channel (90.28 mm). The length of the separation channel from

the intersection point is 80.89 mm. The channels are D-shaped in cross section: 20 μm deep and 50 μm wide at the top (**Figure 4.2.**). Each channel has a 2-mm-diameter, 1.1-mm deep well at each end; the wells are labeled sample reservoir (SR), sample waste (SW), buffer reservoir (BR), and buffer waste (BW) as depicted in **Figure 4.1.**

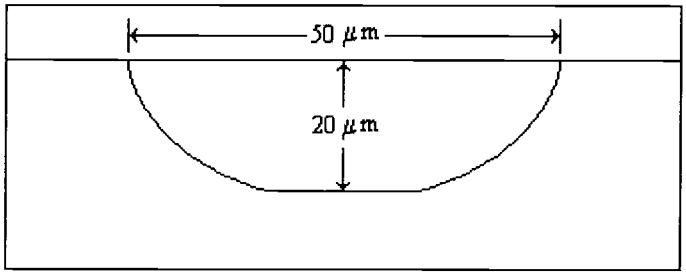

Figure 4.2. Channel cross-section

4.2.3. Chip preparation and storage

To prepare the chip, cleaning fluids were drawn into the chip by applying vacuum to one reservoir and supplying the other three with the appropriate fluid. Chip conditioning consisted of drawing through first 1 M HNO_3, then Millipore water, 1 M NaOH, water again, and finally the running buffer. A 1-mL plastic syringe was used for applying vacuum to one reservoir. When not in use, the chip was immersed in water.

4.2.4. Instrumentation

The instrument used to operate the microchip was the Micralyne Microfluidic Tool Kit (μTK). The μTK is designed to facilitate the operation of electrophoretically based protocols on microchips by providing integrated modular high-voltage (HV) power supplies, a laser-induced fluorescence (LIF) inverted epiluminescence confocal microscope with laser, photomultiplier tube (PMT), a data acquisition board and control software. Safety interlocks on the system prevent the operator from being exposed to HV or laser illumination while protecting the PMT from exposure to overloading signals from external sources.

As configured for these experiments, the HV electronics comprised two HV boards, each of which had two +6 kV power supplies capable of 80 μA, sink or source. The outputs from the HV boards are switched between ground, floating and HV states and are connected to Pt electrodes in a grid above the chip stage. The green LIF used here provides excitation at 532 nm and detection at 570 nm.

The μTK was operated by means of a compiled LabView Interface supplied by Micralyne.

4.2.5. Amino Acid Labeling

Amino acid solutions (10mM) were prepared individually in 0.1 M sodium bicarbonate (pH=8.3). The fluorescent derivatizing reagent, 5-TAMRA-SE, was

dissolved in DMSO at 10mg/ml immediately prior to use. The TAMRA solution was mixed with amino acid solution at a molar ratio 1:10, and the reaction was allowed to proceed at room temperature overnight in the dark with gentle shaking. The labeled samples were diluted 500-fold into the running buffer.

4.2.6. MALDI-TOF MS Experiments

MALDI-TOF MS analyses were performed on an Autoflex II instrument (Bruker Daltonics, Billerica, MA, USA). The MALDI probe was spotted with 1 μL of a 1:1 (by volume) mixture of sample and a saturated solution of a-cyano-4-hydroxycinnamic acid (HCCA) in 50% acetonitrile. The instrument was operated in the positive ion mode with an accelerating potential of 19 kV and an extraction delay of 110 ns. A spectrum was produced by averaging data generated from 80 laser pulses.

4.2.7. CE Experiments

To perform the electrophoretic separations, the channels were filled with a 5 mM sodium tetraborate buffer (pH=9.4) solution. The sample solution was then loaded into position SR and the running buffer to the other three reservoirs, and the chip was ready to run. Solutions were loaded into the reservoirs with a 10μL Eppendorf syringe. The volumes used were 3 μL in each well.

The voltages control and switch programs are shown in **Table 4.1.** The first program step forms a sample plug in the intersection and the second step injects the plug down the separation channel.

	Reservoir potential (kV)				
step	sample	buffer	sample waste	buffer waste	duration (s)
Plug formation	1.5	1.1	GND	1.1	20
Separation	5.2	6	5.2	GND	60

Table 4.1. Two-step High-Voltage Program used to first form a plug of sample at the channel intersection and then to inject it down the separation channel toward the detector.

4.3. Results and Discussion

4.3.1. Amino Acid Fluorescent Labeling

A drawback of fluorescence detection utilizing light sources at wavelengths above 300 nm is the necessity to derivatize most analytes prior to analysis. This can be very challenging, especially at low analyte concentrations or for compounds lacking the appropriate functional groups.

Reactive esters, especially N-hydroxysuccinimide esters, are among the most commonly used reagents for modification of amine groups. Amine-reactive reagents react with non-protonated aliphatic amine groups according to the reaction [7]:

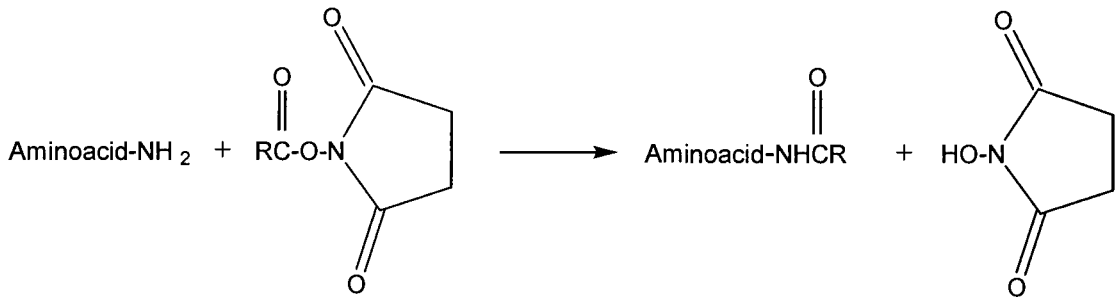

where R is tetramethylrhodamine.

MALDI-TOF mass spectrometry was used to verify the formation of the aminoacid-dye conjugate. Mass spectra presented in **Figure 4.3-5.** confirmed the presence of the conjugates in the labeling cocktail. Also present in all mass spectra is a signal at m/z 431.2 corresponding to the protonated monoisotopic ion of the hydrolyzed dye.

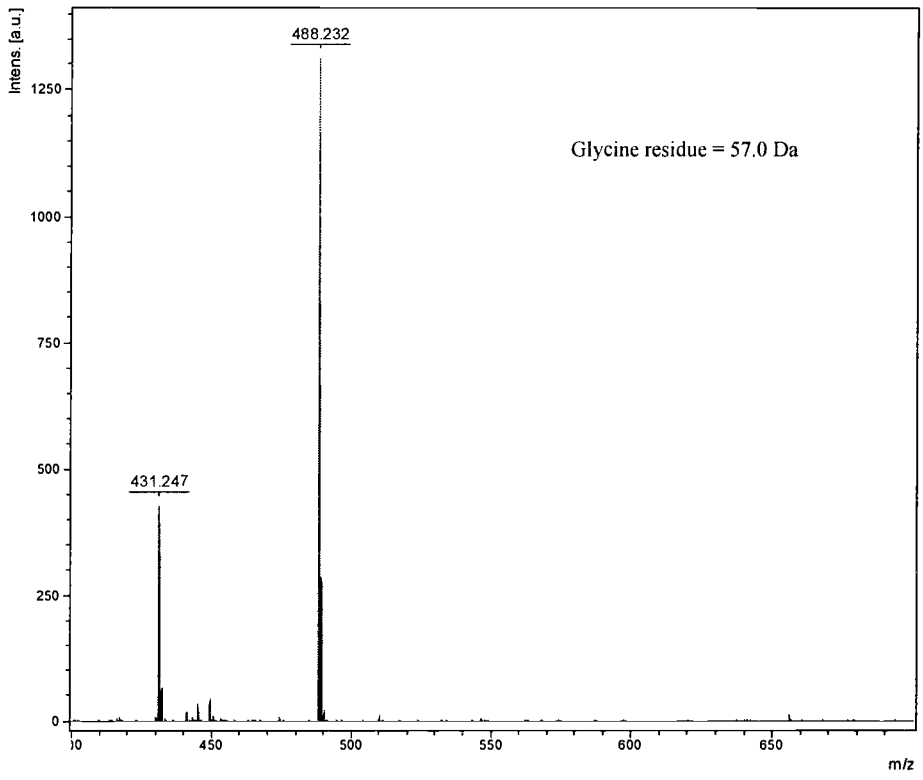

Figure 4.3. MALDI-TOF Mass spectrum of fluorescently labeled glycine. The signal at m/z 431.2 corresponds to the protonated monoisotopic ion of the hydrolyzed dye.

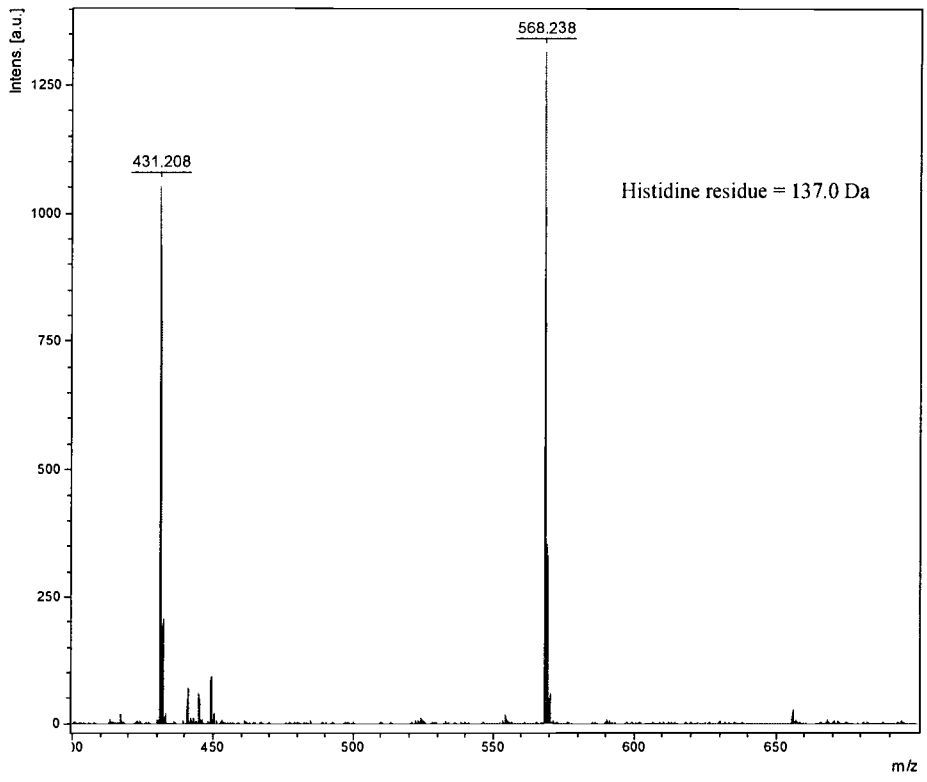

Figure 4.4. MALDI-TOF Mass spectrum of fluorescently labeled histidine. The signal at m/z 431.2 corresponds to the protonated monoisotopic ion of the hydrolyzed dye.

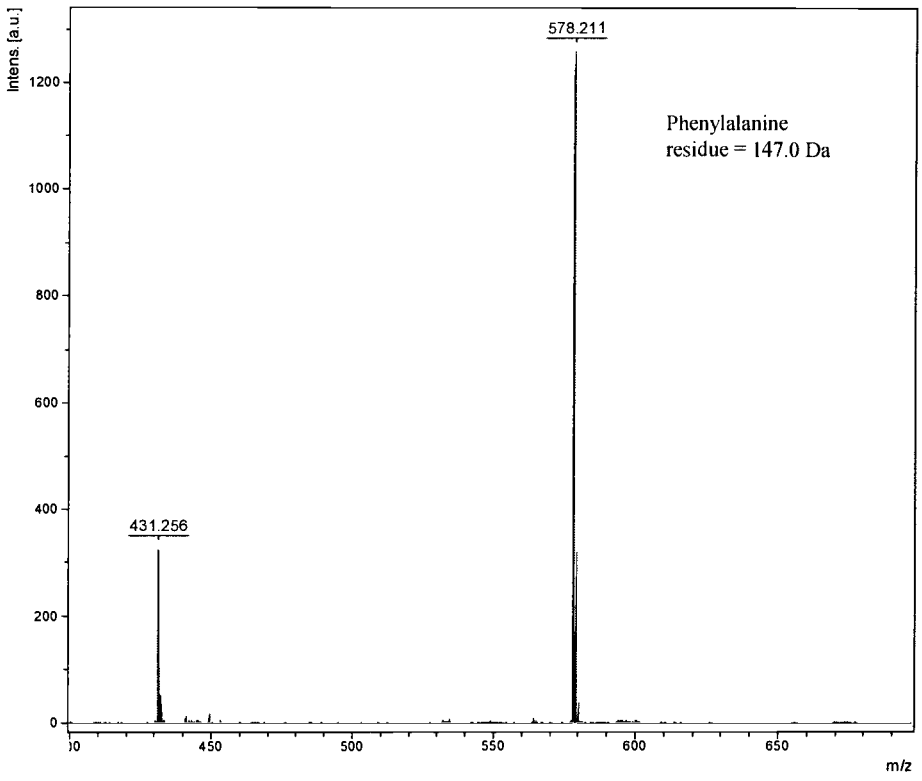

Figure 4.5. MALDI-TOF Mass spectrum of fluorescently labeled phenylalanine. The signal at m/z 431.2 corresponds to the protonated monoisotopic ion of the hydrolyzed dye.

4.3.2. Separation of Amino Acids on Microfluidic Devices

The greatest difference between conventional CE and microchip CE lies in sample injection system. In conventional CE, for sample injection the inlet capillary end is placed in a sample vial and the sample can be injected into the capillary hydrodynamically or electrokinetically. Then the inlet end is placed in a buffer vial and a voltage is applied for separation.

In microfluidic devices, for sample injection, an electric potential is applied between the sample (SR) and sample waste (SW) reservoirs and in this way the sample solution fills the sampling channels through the intersection. Then a potential difference is applied between the buffer (BR) and buffer waste (BW) reservoirs to pull the sample plug at the cross intersection into the separation channel. Due to diffusion and convective flow, leakage of sample solution from the side channels into the separation channel during electrokinetic injection may occur if the separation channel is left floating. The same kind of leakage can also occur in the separation step if the sample channels are left floating. To prevent leakage and to obtain a clearly defined sample injection plug all intersecting channels are under voltage control at all times (see **Table 4.1.**). A well-defined sample plug is formed during injection by applying appropriate voltages at buffer reservoirs inducing counter electrokinetic flows in the separation channel towards the intersection to balance the diffusion and convection effects. For separation, a high voltage is applied along the separation channel while maintaining a small voltage at the sample and sample waste reservoirs. This allows a

sample plug to be pulled into the separation channel while at the same time sample solution in the side channels is kept away from the intersection to avoid leakage of sample into the separation channel.

A variation on the pinched injection described above is the double-T injection, where the two side channels are offset by a certain distance, as illustrated in **Figure 4.1.**, thereby increasing the volume to be injected.

Separation conditions with respect to pH, composition and ionic strength of the running buffer have been optimized for the electrophoretic separation of TAMRA-labeled amino acids. A 5 mM sodium tetraborate buffer (pH=9.4) was chosen as the running buffer for all separations. An example of an electropherogram of three labeled amino acids (Gly-TAMRA, Phe-TAMRA and His-TAMRA) in sodium tetraborate buffer is shown in **Figure 4.6.** As expected, based on the mass spectrometry results, a peak for the hydrolyzed dye is also observed in all electropherograms. Even though after conjugation to the relatively bulky fluorescent dye, the differences in the charge-to-size ratios of the analytes are minimal, a good separation was still obtained.

The electropherogram depicted in **Figure 4.6.** was obtained by positioning the fluorescence detector at L = 20 mm downstream from the injection cross. The electric field strength applied was 660V/cm (6000 V applied between BR and BW reservoirs). The assignment of the various peaks is based on single runs of each of the three amino acids.

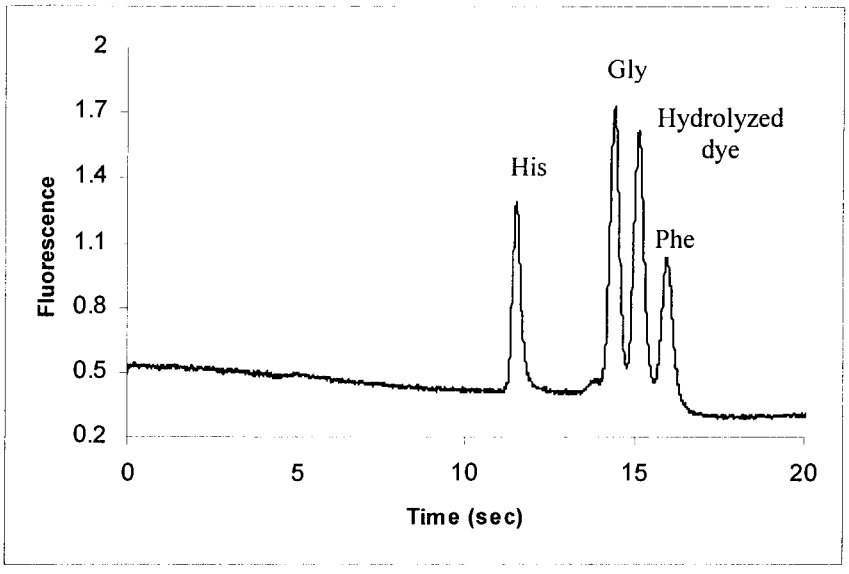

Figure 4.6. Separation and LIF detection of fluorescently labeled amino acids (histidine, glycine and phenylalanine) at a concentration of 0.7 μM. The separation buffer was 5 mM sodium tetraborate (pH=9.4). Effective separation length = 20 mm. Electric field strength = 660 V/cm.

In capillary electrophoresis, the efficiency of a separation is defined as:

$$N = \frac{\mu \cdot V}{2D_m} \qquad (4.1)$$

where D_m is the diffusion coefficient of the analyte and μ is the apparent mobility of the solute in the separation medium. Equation 4.1 predicts that efficiency is only diffusion-limited and increases directly with field strength. Since separations in

miniaturized devices usually take less then 1 minute, band-broadening due to longitudinal diffusion is insignificant, and extremely high efficiencies are observed in microchip electrophoresis.

Plate numbers, calculated using the peak width at half-height, $w_{1/2}$ (s) formula [8]:

$$N = 5.54 \cdot \left(\frac{t_r}{w_{1/2}} \right)^2 \qquad (4.2)$$

varied from N = 5.4 x 10^5 plates/m for histidine to a maximum of N = 6.4 x 10^5 plates/m for glycine.

The sample volume injected in the separation channel was ~ 100 pL, and therefore at a concentration of 7 μM, the detected amounts of the TAMRA-labeled amino acids are approximately 7 attomoles.

4.3. Conclusion

Electrophoretic separations of amino acids on a glass microchip have been achieved within 1 minute with high separation efficiency and detection limits in the attomoles range.

Integration of a sample injector based on a volume-defined injection scheme allows reproducible introduction of very small sample volumes of about 100 pL. Reproducibility of the migration times and the peak areas is reasonably good.

Fluid flow can be easily and effectively controlled on these devices by switching of electric potentials. The fact that no external pumps and valves are required makes this technique particularly suitable to automation and miniaturization.

References:

1. Manz, A.; Graber, N.; Widmer, H.M. *Sens. Actuators, B Chem.*, B1, (1-6), **1990**, 244.

2. Manz, A.; Harrison, D.J.; Verpoorte, E.; Widmer, H.M. *Advances in Chromatography*, Brown P.R.; Grushka, E., **1993**, 1.

3. Dolnik, V; Liu, S.; Jovanovich, S. *Electrophoresis*, **2000**, *21*, 41.

4. Bruin, G.J.M. *Electrophoresis*, **2000**, *21*, 3931.

5. Reyes, D.R.; Iossifidis, D.; Auroux, P.-A.; Manz, A. *Anal. Chem.*, **2002**, *74*, 2623.

6. Vilkner, T.; Janasek, D.; Manz, A. *Anal. Chem.*, **2004**, *76*, 3373.

7. Brinkley, M. *Bioconjugate Chem.*, **1992**, *3*, 2.

8. Snyder, L.R.; Kirkland, J.J. *Introduction to Modern Liquid Chromatography*, 2nd Edition, John Wiley & Sons, New York, **1979**, Chapter 5.

CHAPTER 5

PROGRESS TOWARDS THE DEVELOPMENT OF IMMOBILIZED STATIONARY PHASES FOR MICROCHIP DEVICES

5.1. Introduction

As discussed in Chapter 4, microfluidic devices have been fabricated using various glass substrates. The preference for glass substrates is attributed to their favorable optical properties, well-understood surface chemistry, and well-developed microfabrication methods, adapted from the microelectronics industry. However, the fabrication of glass devices is often expensive, time-consuming, requires special equipment, and is laborious.

Polymer materials have been embraced as perhaps the most attractive alternative to conventional glass for fabrication of microfluidic systems. Compared to glass and silicon, polymer microchip manufacturing procedures are simpler and cheaper. The basic concept of these manufacturing techniques is the replication of a microfabricated mold tool, which represents the negative (inverse) image of the desired polymer structure. The expensive microfabrication step is therefore necessary only once for the fabrication of this master structure, which then can be replicated many times into the polymer substrate.

One particular advantage to using polymers is the large variety of materials available (in terms of their physical and chemical characteristics), which makes them suitable for different kinds of microfluidic applications.

Poly(dimethylsiloxane) (PDMS) has been one of the most actively investigated materials for microfluidics [1-3]. The soft lithography technique used for PDMS chip fabrication allows rapid prototyping of the microchips. However, PDMS has drawbacks including high gas permeability, a tendency to swell in certain organic solvents, high hydrophobicity and lack of surface charge required to generate and support electroosmotic flow.

Various energy sources such as oxygen plasma, UV light and corona discharges have been used to modify the surface properties of PDMS microchips. Unfortunately, the surface of oxidized PDMS is known to recover its hydrophobicity within a short period of time after oxidation. Further modification of the oxidized surface with various derivatization agents may prevent its reversion, as described herein, making PDMS a more viable selection for use with wall-anchored monolithic sorbents.

Another polymer that has seen much attention is polycarbonate [4-6]. Polycarbonate (PC) lends itself readily to microfabrication via hot embossing and injection molding. However, like PDMS, polycarbonate is very hydrophobic. The polycarbonate surface does not have many ionizable chemical functional groups and, therefore, exhibits very weak electroosmotic flow [7]. A novel solution to this problem

is to coat the polycarbonate surface with a thin layer of silicate. The resulting glass-like surface is easy to derivatize with different functionalities.

High-performance separation systems are critical to the success of μ-TAS. At the present time, on-chip separations are dominated by electrophoretic methods. However as the field of μ-TAS develops there is a growing demand for additional modes of separation, especially chromatographic modes, in order to resolve increasingly complex samples.

A promising alternative to electrophoresis is electrochromatography, a technique that combines feature of both electrophoresis and liquid chromatography. Despite remarkable progress, the field of microchip electrochromatography is still in its infancy. A great effort is currently focus on developing new methods that enable the introduction of stationary phase within the channels of a microfluidic device.

Porous monolithic polymers have been successfully employed as stationary phases for both liquid chromatography and capillary electrochromatography [8-10]. The continuous bed is prepared by the copolymerization of a mixture of monomers in the presence of a porogenic solvent. There are several advantages to this approach. The tedious and irreproducible process of frit fabrication and packing is avoided by the simple *in situ* polymerization procedure. A broad variety of commercially available monomers offer flexibility in tailoring the surface chemistry.

Although a few applications involving monolithic polymers have been demonstrated on microfluidic devices [11-15], the majority of the applications of monolithic sorbents were performed in capillary columns.

Numerous papers have already demonstrated the use of PDMS chips as open channel separation devices [16-21]. However, there are only a few reports of attempts to increase the limited surface area of these channels by classical approach of packing particles into the channel [22,23] or by molding collocated monolithic support structures (COMOSS) directly in the channel [24,25].

Given the notoriously poor compatibility of many polymeric materials, it is likely that poor bonding of the monoliths to the native walls of plastic devices will be observed, and that voids may even develop at the monolith-channel interface making the devices ineffective. Therefore, the plastic channel surface must be modified prior to the *in situ* preparation of the monolith in order to anchor the monolith in place.

The main goal of this preliminary study is to develop a surface modification method that makes possible the anchoring of the polymeric monolith to the walls of the microchip. Continuous polymeric beds are prepared within a channel of three different microchip substrates: glass, poly(dimethylsiloxane) and polycarbonate. The methacrylate-based monolith is cast *in-situ* via UV-initiated polymerization. The functionalization of the inner wall of the channel with methacryloyl groups enabled the covalent binding of the monolith to the wall. The morphology of the wall-anchored monolith is confirmed by SEM of chip sections, and by SEM of an extruded segment of non-anchored monolith from a separate chip.

5.2. Experimental Section

5.2.1. Chemicals and materials

Butyl methacrylate (BMA), ethylene dimethacrylate (EDMA), 2-acrylamido-2-methyl-propansulfonic acid (AMPS), 2,2-dimethoxy-2-phenyl-acetophenone (99%, DMPAP) and [(methacryloxy)-propyl] trimethoxysilane were purchased from Aldrich (Milwaukee, WI, USA) and used as received. The solvents employed were HPLC grade and were purchased from Fisher Scientific (Pittsburgh, PA, USA).

Sylgard 184 silicone elastomer and curing agent were purchased from Dow Corning Corporation (Midland, MI, USA).

5.2.2. Microchip layout and fabrication

In the next sections, different methods for chip fabrication are presented, as well as the chip layouts.

5.2.2.1. Glass microchip

The glass microchips were purchased from Micralyne Inc. (Edmonton, AB, Canada). The layout of the glass microchip was presented in **Chapter 4.** Each microchip device is 16 x 95 x 2.2 mm and made from 2 fused pieces of low

fluorescence Schott Borofloat™ glass. Each plate is 1.1 mm thick with the bottom plate containing the etched pattern and the top plate containing the reservoir holes. The microchips consist of a cross-shaped intersection of an injection channel (9.64 mm) and a separation channel (90.28 mm). The length of the separation channel from the intersection point is 80.89 mm. The channels are D-shaped in cross section: 20 μm deep and 50 μm wide at the top (**Figure 4.2.**). Each channel has a 2-mm-diameter, 1.1-mm deep well at each end.

5.2.2.2. PDMS microchip

The microfluidic channel patterns in PDMS were prepared by means of soft lithography, as shown schematically in **Figure 5.1.** The first task in producing a PDMS microchip is the fabrication of a master. We used two different approaches to obtain a master. For purpose of rapid prototyping, a straight channel master was manufactured from a Teflon sheet using a CNC milling machine. For more intricate designs, SU-8 25 negative photoresist was spin-coated on a 3 in. silicon wafer at 1000 rpm to reach the desired thickness of 100 μm. The photoresist was pre-baked onto the silicon wafer at 90°C. The photoresist was then patterned by exposing it to UV radiation through a photolithography mask. Following UV exposure, the wafer was subjected to a post-exposure bake at 95 °C for 5 min. The wafer was then immersed into an SU-8 developing solution for a period of time sufficient to remove unmodified photoresist, leaving the bare silicon surface. Areas of photoresist chemically modified

by the ultraviolet light were resistant to the developing solution leaving raised structures corresponding to the desired pattern.

Microchips were fabricated using replica molding [16]. Sylgard 184 PDMS prepolymer was mixed thoroughly in a 10:1 mass ratio of silicone elastomer to curing agent, degassed and poured onto the master. Chips were cured at 65°C for 24h. After curing, the PDMS replica was peeled from the mold and holes were punched into the polymer to create access ports. Flat PDMS substrates were obtained by casting prepolymer mixture against a clean glass plate and curing.

The two pieces of PDMS were placed in an oxygen plasma and oxidized for 1 min. When joined together, the oxidized parts sealed irreversibly.

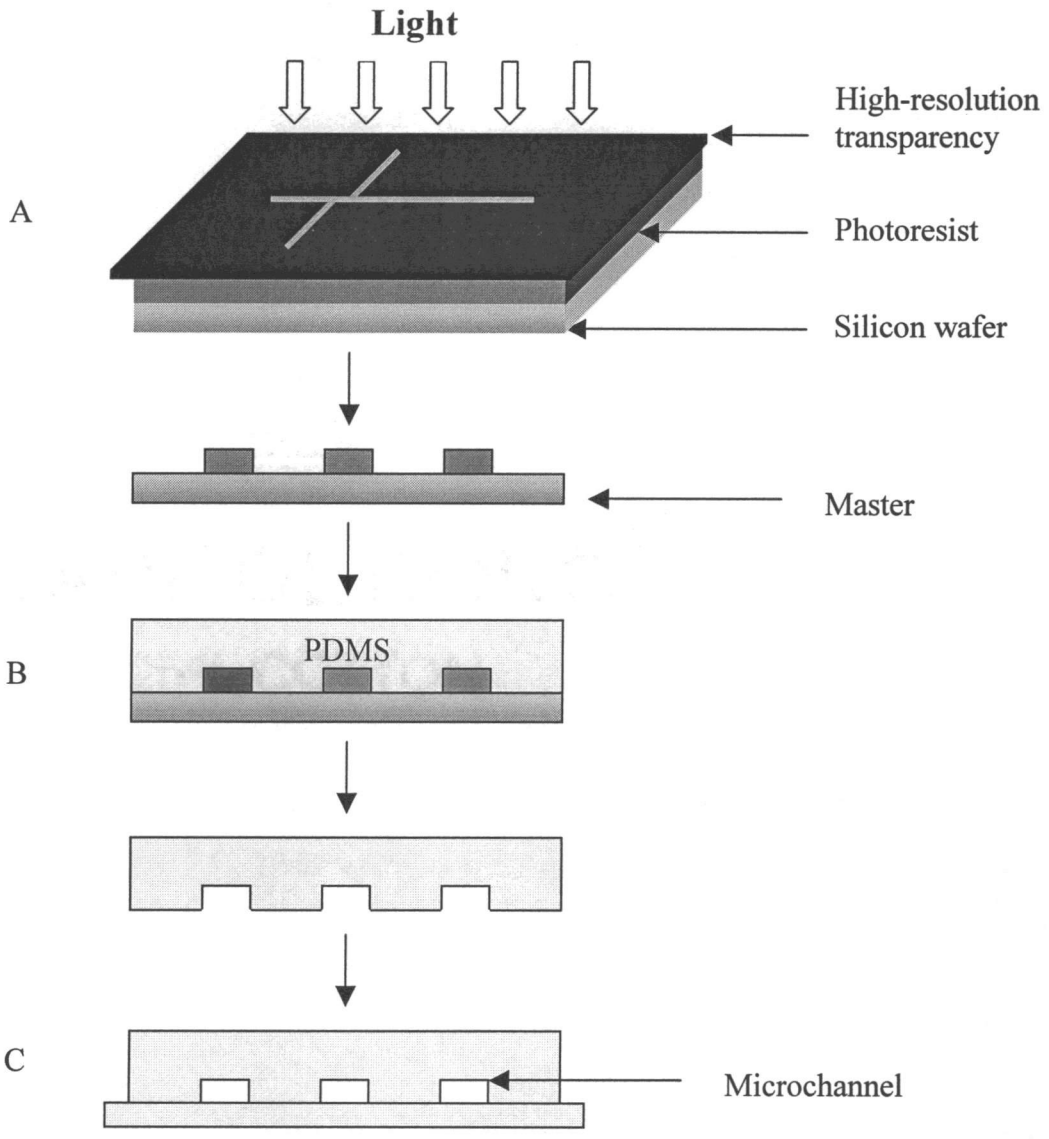

Figure 5.1. Illustrative scheme of PDMS device fabrication by photolithography and replica molding.

5.2.2.3. Polycarbonate microchip fabrication

PC microchips were fabricated by hot embossing the polycarbonate substrate onto a nickel-on-stainless-steel mold. The mold was produced using electroplating methods. Electroplating (or electrodeposition) is a process typically used to obtain thick (tens of micrometers) metal structures. The process starts with a photolithographic step, in which a SU-8 photoresist-coated substrate is exposed to light through a photomask and subsequently developed, so that the areas to be electroplated are free of resist. The structure is then placed in a Ni sulfamate galvanic bath. The Ni ions are reduced at the substrate surface, and the metal starts to grow in the resist structure. After the resist structure is overgrown with the metal, the photoresist is dissolved and the resulting master can be used for replication. A schematic of the fabrication process is presented in **Figure 5.2.**

Photomasks (**Figure 5.3.**) used for fabrication of both molds were designed in-house using CANVAS 8.0 (Deneba) software and printed on 8 mil transparencies at 8000 dpi resolution (Artnet Pro, Inc., San Jose, CA, USA).

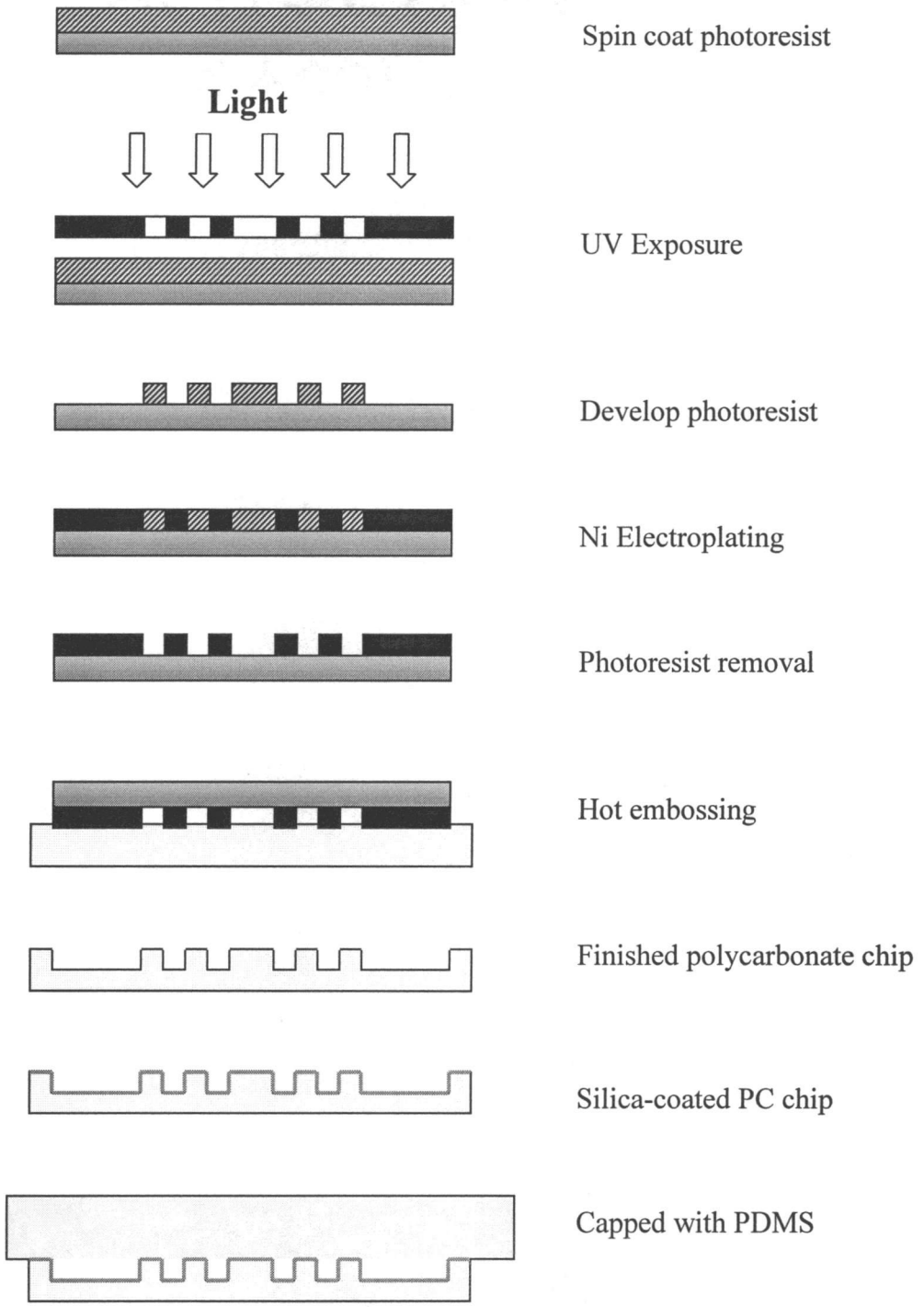

Figure 5.2. Illustrative scheme of polycarbonate microchip fabrication

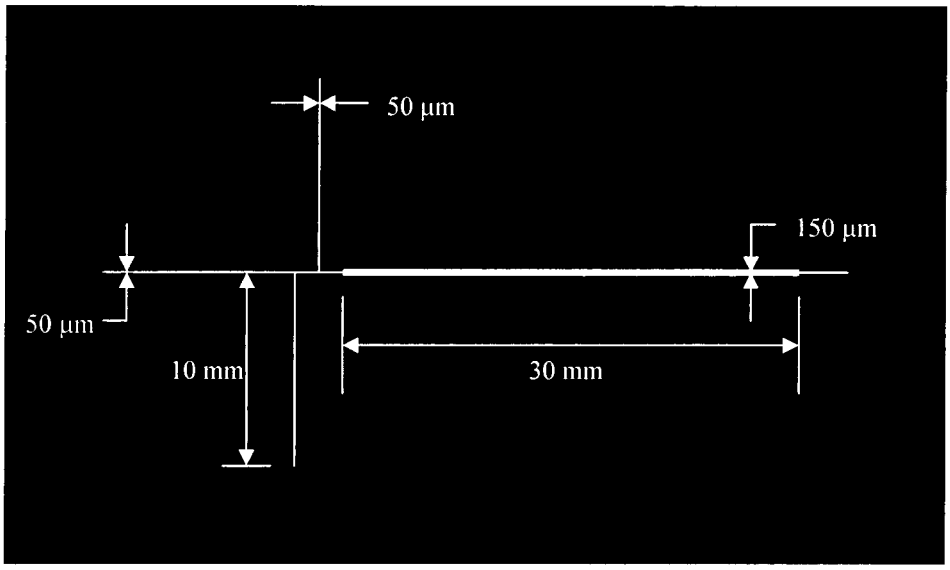

Figure 5.3. High-resolution transparency photomask used for fabrication of master molds

5.2.3. Pretreatment and surface derivatization of the microchannels

Glass microchannels were simply rinsed with 1 M NaOH solution for 10 min, deionized water, and acetone before surface derivatization.

For PDMS substrates, the upper and lower portions of the chip were first exposed to plasma oxidation and the microchannel formed between the two layers was immediately filled with the derivatization mixture.

PC substrates containing microfluidic features were sputter coated (Veeco Ion Beam Sputtering System) with a thin layer (~0.1 μm) of silicon dioxide (Kurt J.

Lesker Co., Clairton, PA, USA). The silica coated PC substrate was then sealed against a plasma oxidized flat piece of PDMS to form the microfluidic channel.

The inner walls of all microchips were functionalized with [(methacryloxy)-propyl] trimethoxysilane, using a method adapted from Hjertèn [26]. The channel was filled with a 30% solution of [(methacryloxy)-propyl] trimethoxysilane in acetone. The solution was kept in the channels for 1+ hours. The channels were then flushed with distilled, deionized water and finally purged and dried with a flow of nitrogen.

5.2.4. Monolithic rod preparation

DMPAP (1 wt % with respect to the monomers) was dissolved in a monomer mixture consisting of 40% EDMA, 59.7% BMA and 0.3% AMPS. The solvent, a mixture of isopropanol, 1,4-butandiol and water (6:3:1 v/v/v), was slowly admixed to the monomers in a 2:3 (v/v) ratio. The homogeneous mixtures were purged with nitrogen for 5 min. The channels were filled with the polymerization mixture using a 100 μL syringe. Polymerization was initiated by UV irradiation for 20 min under a UV lamp (Spectroline X-15A, Spectronics Corporation, Westbury, NY, USA). Examination of channels during monolith preparation was achieved with a simple Stereomaster optical microscope (Fisher Scientific, Houston, TX, USA) with 40X magnification. The morphology of the monoliths was studied using an AmRay (Bedford, MA, USA) scanning electron microscope (SEM) operated at 10 kV.

5.2.5. Contact angle measurements

Contact angles were measured on flat surfaces of different substrates before and after surface derivatization. A droplet of deionized water was placed on the surface at room temperature, and after 20 sec the contact angle was measured using a contact angle goniometer (First Ten Ängstroms, Portsmouth, VA, USA). The contact angles reported are averages of at least five measurements.

5.3. Results and Discussion

The primary goal of this research work was to develop a method for casting and immobilizing polymer monoliths inside channels on various microchip substrates.

Our approach to prepare the monoliths is to functionalize the wall surface using [(methacryloxy)-propyl] trimethoxysilane. During the course of the subsequent polymerization, this surface modification will facilitate the covalent bonding of the porous monolith to the channel walls, thus anchoring and stabilizing the monolith.

The necessity of anchoring the monolith to the wall is demonstrated by the scanning electron micrograph (SEM) presented in **Figure 5.4.** that shows a large void between the PDMS and the unmodified microchip wall due to the shrinking of the monolith.

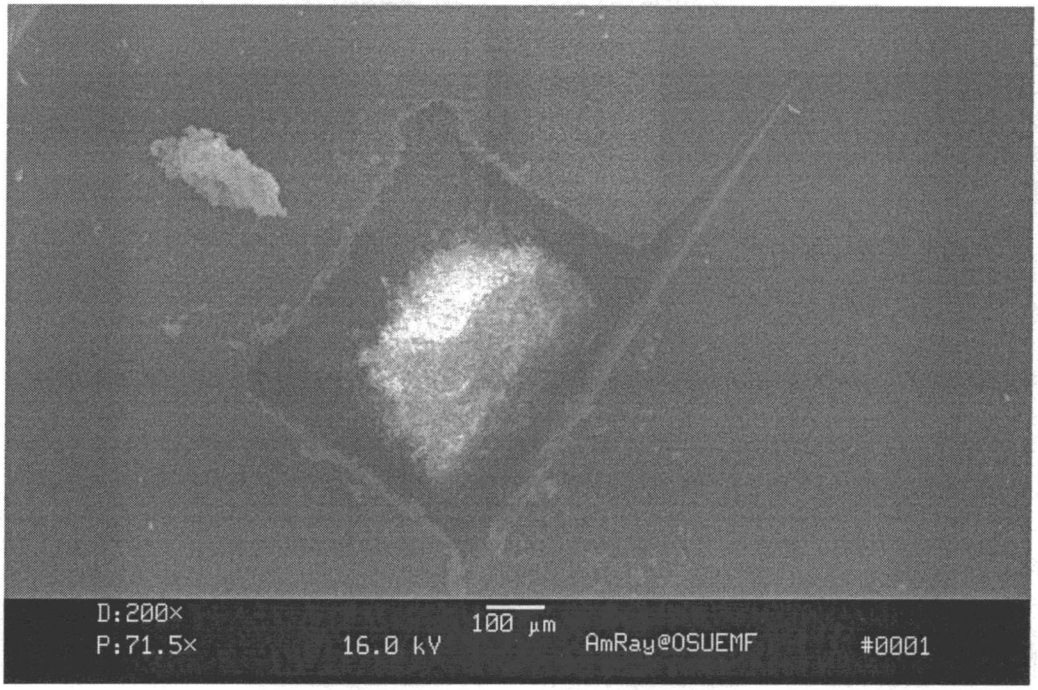

Figure 5.4. SEM image of a methacrylate-based monolith prepared inside an unmodified PDMS microchip. Note shrinkage and contraction of the polymer, leading to large voids at the walls.

For glass microchips, surface silanization and monolith polymerization is a relatively easy and straightforward procedure transferred from capillary format. **Figure 5.5.** shows an SEM image of a channel in the microchip containing photopolymerized porous polymer monolith. The characteristic D-shape of the glass channel is due to isotropic etching. The polymer is cast uniformly over the cross section of the channel and is covalently bonded to the wall. Physical characterization of the porous polymer monoliths is provided in Chapter 3.

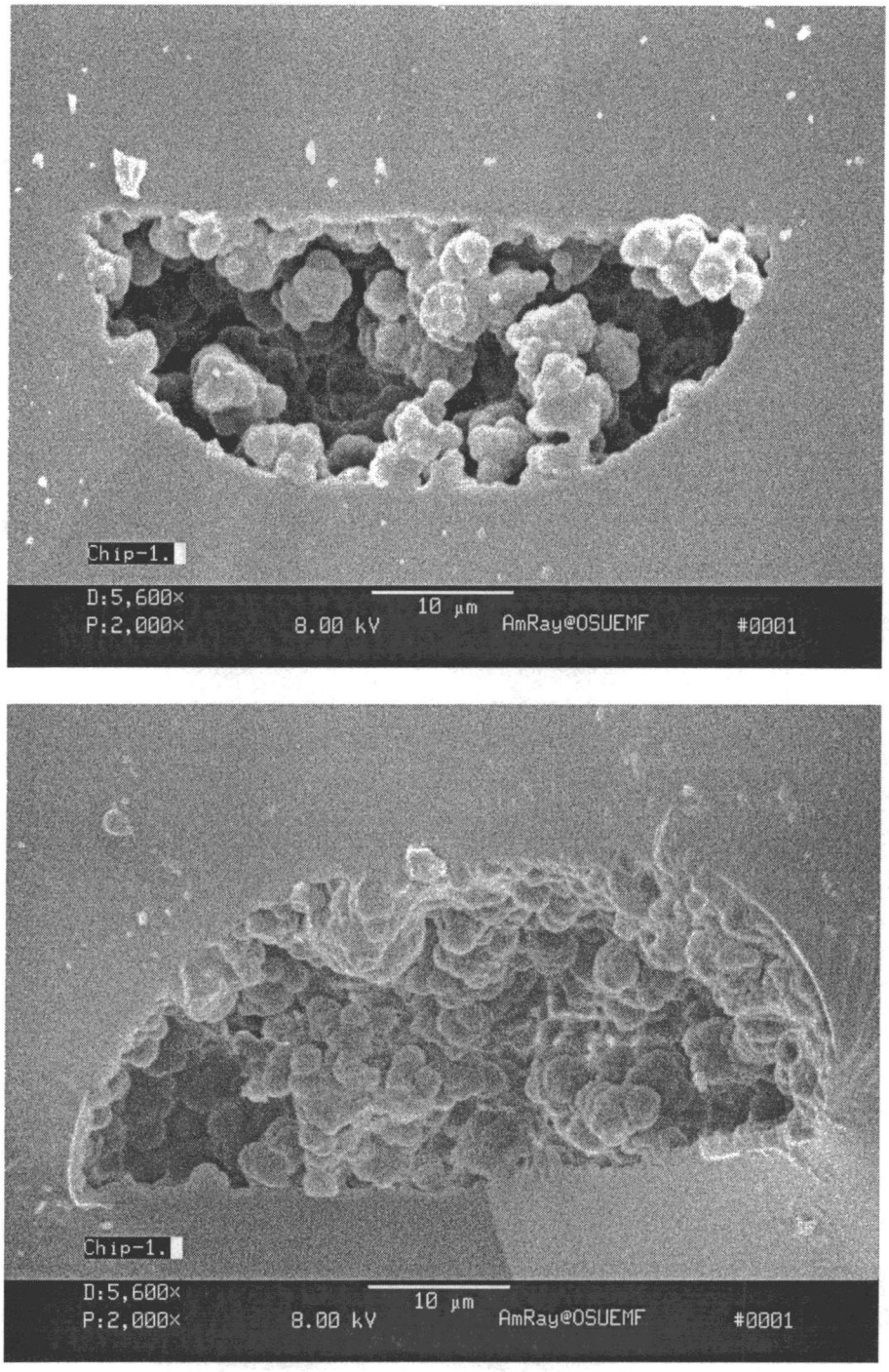

Figure 5.5. SEM images of porous polymer monolith inside a glass microchip

It is known that the native PDMS surface is highly hydrophobic. The PDMS surface can be made hydrophilic by exposure to an oxygen plasma. Oxygen plasma treatment transiently modifies the PDMS to a more silica-like surface chemistry [27, 28]. This allowed the channel walls to be modified using variations on procedures well established for derivatization of silica-based materials. As for glass microchips, the agent of choice was [(methacryloxy)-propyl] trimethoxysilane.

The contact angle measurement of a water droplet is frequently used as a measure of the hydrophobicity of a surface [29,30]. The average water contact angle for pristine PDMS was found to be 108^{o}, a value consistent with the hydrophobic nature of PDMS. Immediately after plasma oxidation, the contact angle of water dropped to 23^{o}. However, water contact angle measurements demonstrated that the surface treated with oxygen plasma recovered hydrophobicity in a matter of 1-2 days.

In contrast, for a piece of PDMS that was plasma oxidized and immediately derivatized with [(methacryloxy)-propyl] trimethoxysilane, a water contact angle of 60^{o} was maintained for 2 weeks.

Following derivatization of the channel surfaces, monolithic porous polymers were prepared in situ on the microchip by photoinitiated polymerization. Due to the relatively large size of the channel, the SEM images of the cross-sectional view of the channel are of modest diagnostic value; the elasticity of the PDMS made it difficult to obtain a clean cut of the microchip and yielded damage to the monolith. **Figures 5.6.a** and **5.6.b** present the channel cross sections of a chip fractured at room temperature (a) and after being frozen in liquid nitrogen (b). A closer look at the monolith near the

channel wall reveals a good adherence to the surface of the wall. Aside from this, the SEM images presented in **Figures 5.7.a** and **5.7.b** indicate a uniform structure of the monolith close to the walls, similar to that in the bulk material.

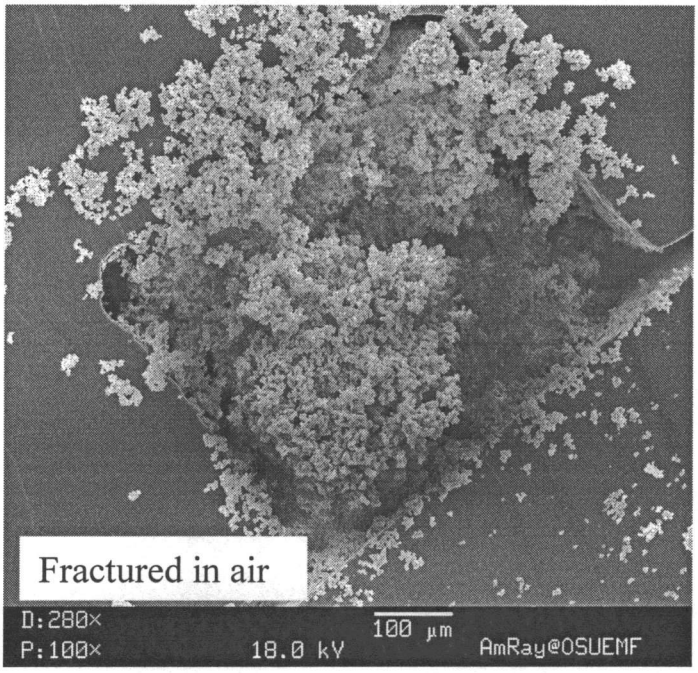

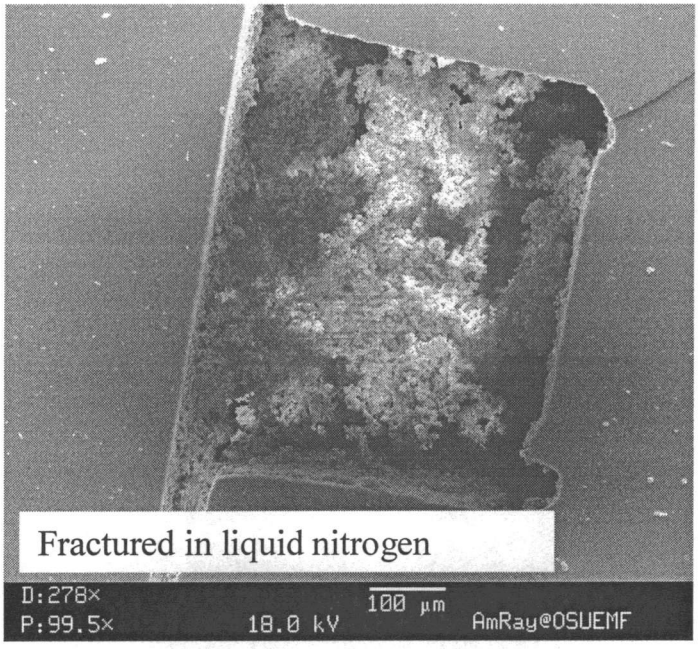

Figure 5.6 a and 5.6 b. SEM images of the channel cross section fractured (a) in air and (b) in liquid nitrogen.

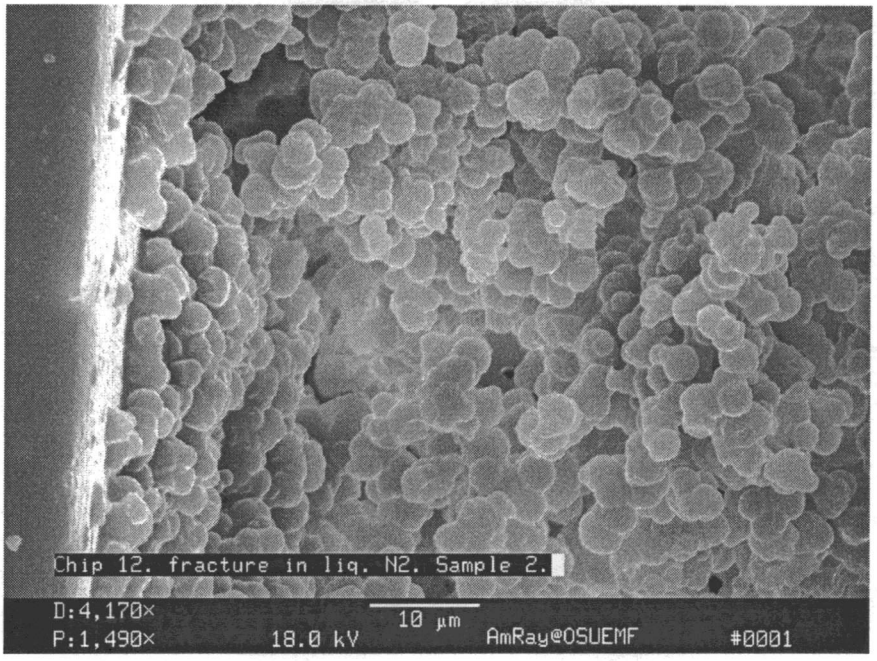

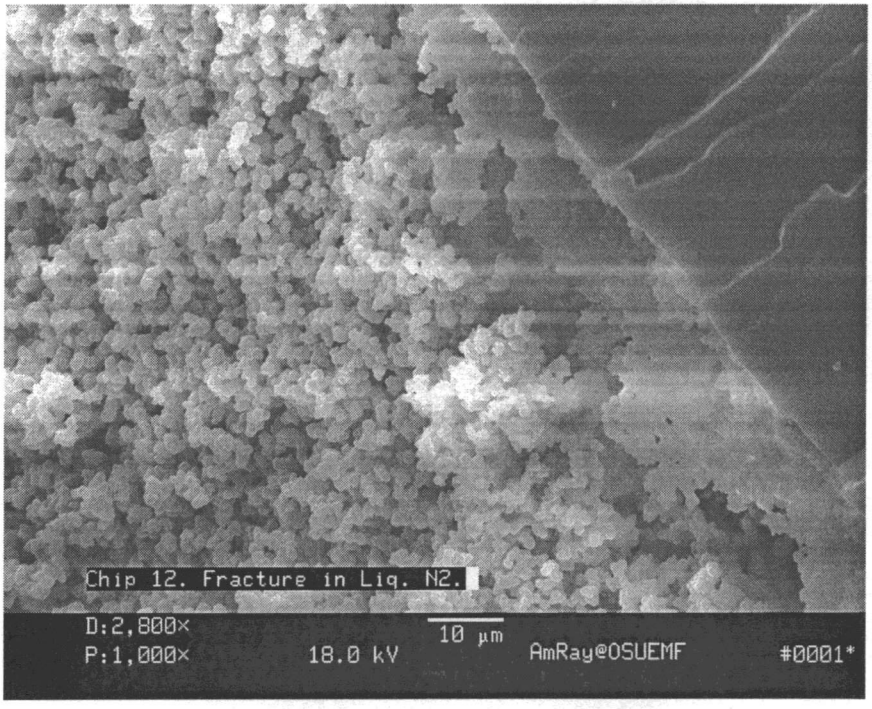

Figure 5.7 a and 5.7 b. SEM images of the wall-anchored porous polymer monolith in PDMS

The monoliths that were not anchored to the microchip walls were readily extruded from the channel and used for morphologic characterization of the monoliths themselves. The polymer was sputter-coated with gold and examined with a scanning electron microscope. The axial and radial images presented in **Figure 5.8.** suggest a highly uniform and permeable structure.

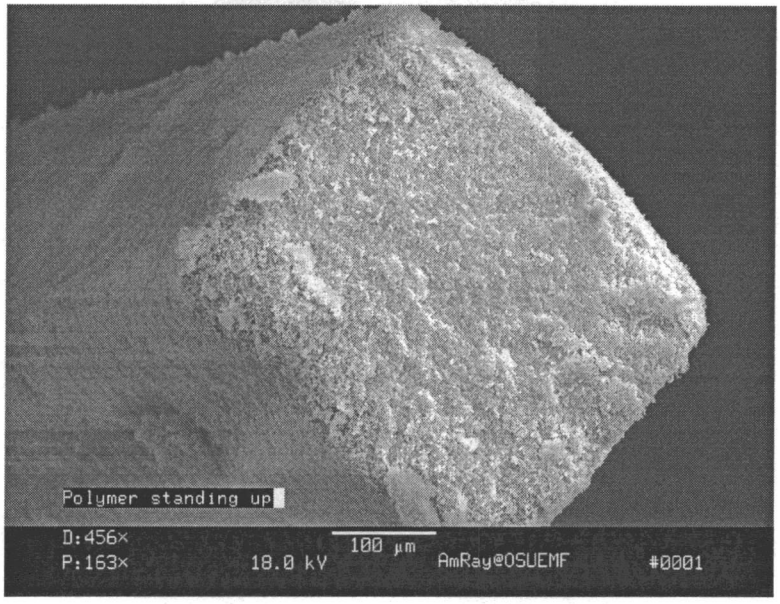

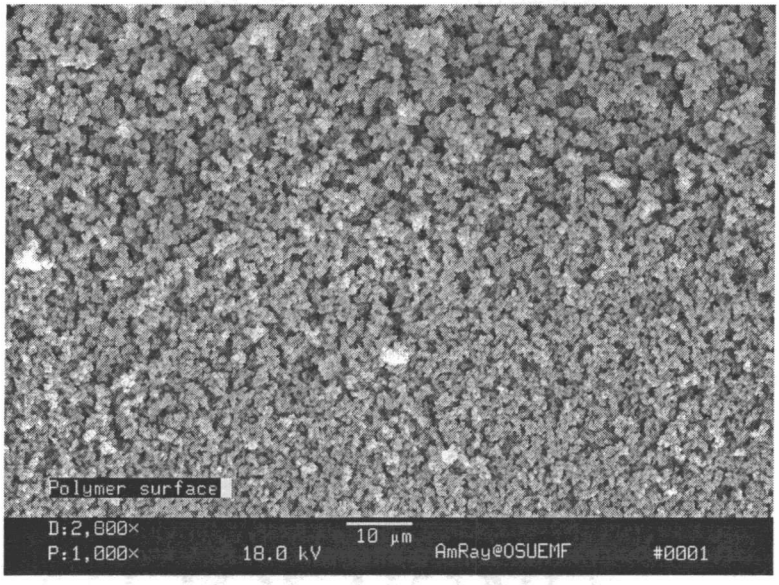

Figure 5.8 a and 5.8 b. SEM images of the (a) axial and (b) radial view of the extruded monolith (cast in PDMS)

Unfortunately, a plasma oxidation process is not adequate to alter the hydrophobic character of polycarbonate surface. In this case, a more sophisticated, but also more efficient procedure to convert the PC into a hydrophilic surface was explored. Thin-film deposition is a method used extensively in semiconductor industry. In sputtering deposition, a target of the material to be deposited (in our case, silicon dioxide) is bombarded with high-energy inert ions (argon). The outcome of the bombardment is that individual atoms or clusters are removed from the target surface and ejected toward the rotating PC substrate where they are deposited. Gradually, a thin film of silica is built onto the polycarbonate substrate.

The formation of the silica layer was confirmed by water contact angle measurements. A water contact angle of 85^{o} was observed for native polycarbonate. After sputtering with silica the contact angle measured was 17^{o} comparable with the water contact angle for glass substrates.

The thickness of the silica layer was estimated to be in average ~ 100 nm.

Subsequently, silica-coated polycarbonate is sealed against a plasma-oxidized layer of PDMS to form a channel. Silanization of the channel walls using [(methacryloxy)-propyl] trimethoxysilane allows the covalent attachment of the polymer monolith.

Figure 5.9. presents the SEM image of a porous polymer monolith inside a channel of a polycarbonate microchip after removal of the PDMS capping layer.

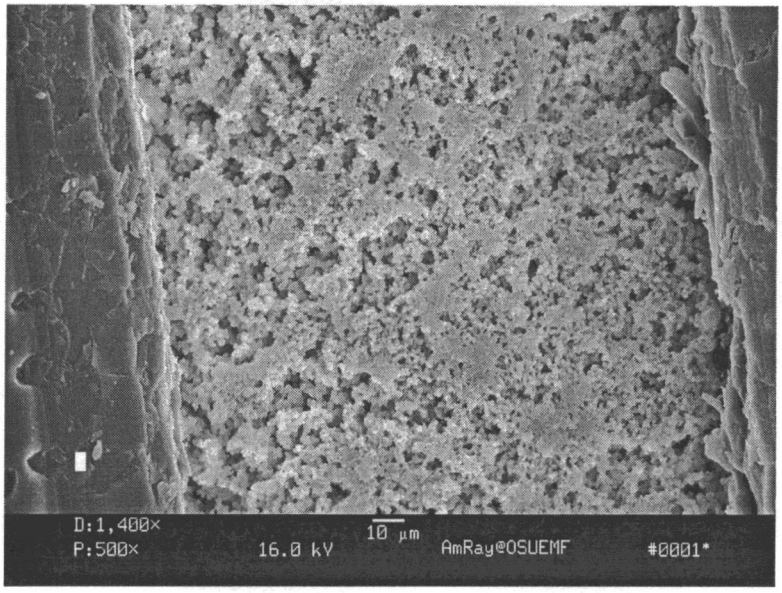

Figure 5.9. SEM images of the wall-anchored porous polymer monolith in a polycarbonate microchip.

The ability to use UV light for initiation of polymerization allows patterning of the chromatographic phase in the channels of a microfluidic chip for optimization of specific functions in the microchip. Using a mask, the polymerization is restricted to UV-exposed regions and monomers from the unexposed regions are flushed after irradiation step. **Figure 5.10.** shows creation of a window that is kept void of polymer for allowing sensitive detection using laser-induced fluorescence. Most of the organic polymers fluoresce to some extent and, combined with scattering, lead to a higher fluorescence background. Also, using photopattering, the injection channels can

remain open, which allows rapid and repeatable injection, and easy cleanup of injection arms.

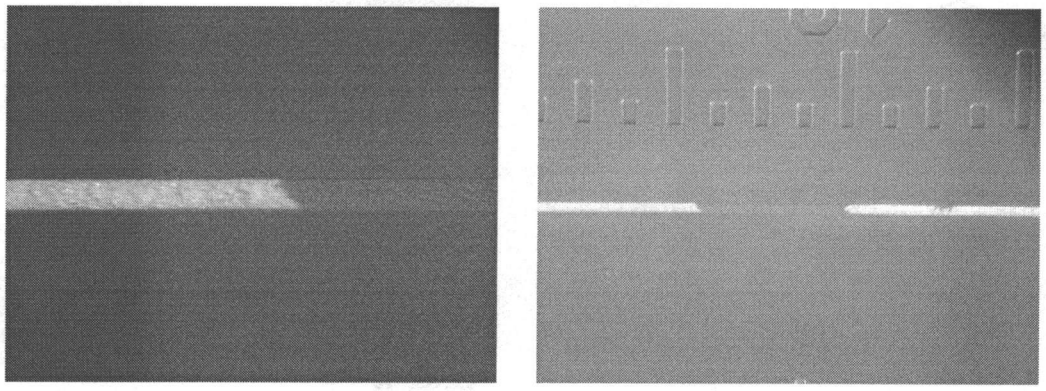

Figure 5.10. Photopatterning of the polymer in microchannels. The polymer was patterned using a mask and a UV lamp.

5.3. Conclusion

A distinct advantage of polymer monolithic stationary phases over packed chromatographic beds is the ability to prepare them easily and rapidly via free radical polymerization within the channels of a microdevice. Adjusting the composition of the initial monomer solution and the polymerization conditions can control the porosity, surface area, and pore size of the monolith.

The first polymer-based monolithic stationary phases were prepared in glass microchips. Before formation of the monolith, the channels were treated with [(methacryloxy)-propyl] trimethoxysilane to facilitate anchoring of the polymer to the walls of the channel.

Although PDMS is a useful material for rapid prototyping purposes, its limited compatibility with many analytes and organic solvents has limited the scope of its application. Modification of surface chemistry is essential in PDMS devices if this promising material is to see expanded utility in the chip-based analytical device community.

A method to derivatize the PDMS surface and to create porous monolithic sorbents on a PDMS microchip has been developed, and SEM imagery has confirmed that the polymer is indeed wall-anchored.

Encouraged by the results obtained for PDMS, another polymer, polycarbonate, has been explored as a material for microchip fabrication. In this case, physical deposition of a thin layer of silica converted the hydrophobic polycarbonate surface into a glass-like material. This allowed the covalent attachment of the polymeric monolith to the channel walls.

Spatial control over polymerization will allow one to create chips with multiple channels containing different separation matrixes to achieve multidimensional separation.

References:

1. McDonald, J. C.; Whitesides, G. M. *Acc. Chem. Res.*, 2002, *35,* 491.

2. Ng, J. M. K.; Gitlin, I.; Stroock, A. D.; Whitesides, G. M. *Electrophoresis*, 2002, *23*, 3461.

3. Sia, S. K.; Whitesides, G. M. *Electrophoresis*, 2003, *24*, 3563.

4. Liu, Y.; Ganser, D.; Schneider, A.; Liu, R.; Grodzinski, P.; Kroutchinina, N. *Anal. Chem.*, 2001, *73*, 4196.

5. Xu, Y. Vaidya, B.; Patel, A.B.; Ford, S.M.; McCarley, R.L.; Soper, S.A. *Anal. Chem.*, 2003, *75*, 2975.

6. Chen, J.; Wabuyele, M.; Chen, H.; Patterson, D.; Hupert, M.; Shadpour, H.; Nikitopoulos, D.; Soper, S.A. *Anal. Chem.*, 2005, *77*, 658.

7. Soper, S.A.; Ford, S.M.; Qi, S.; McCarley, R.L.; Kelly, K.; Murphy, M.C. *Anal. Chem.*, 2000, *72*, 642A.

8. Svec, F., Peters, E.C., Sýkora, D., Fréchet, J.M.J. *J. Chromatogr. A*, 2000, *887*, 3.

9. Svec, F., Peters, E. C., Sýkora, D., Yu, C., Fréchet, J.M.J., *J. High Resol. Chromatogr.*, **2000**, *23*, 3.

10. Hilder, E. F.; Svec, F.; Fréchet, J.M.J. *Electrophoresis*, **2002**, *23*, 3934.

11. Ericson, C.; Holm, J.; Ericson, T.; Hjertèn, S. *Anal. Chem.*, **2000**, *72*, 81.

12. Ngola, S. M.; Fintschenko, Y.; Choi, W-Y.; Shepodd, T. J. *Anal. Chem.*, **2001**, *73*, 849.

13. Yu, C., Davey, M. H.; Svec, F.; Fréchet, J.M.J. *Anal. Chem.*, **2001**, *73*, 5088.

14. Throckmorton, D. J.; Shepodd, T. J.; Singh, A. K. *Anal. Chem.*, **2002**, *74*, 784.

15. Lazar, I. M.; Li, L.; Yang, Y.; Karger, B. L. *Electrophoresis*, **2003**, *24*, 3655.

16. Duffy, D. C.; McDonald, J. C.; Schueller, O. J. A.; Whitesides, G. M. *Anal. Chem.*, **1998**, *70*, 4974.

17. Chan, J. H.; Timperman, A. T.; Qin, D.; Aebersold, R. *Anal. Chem.*, **1999**, *71*, 4437.

18. Ren, X.; Bachman, M.; Sims, C.; Li, G.P.; Allbritton, N. *J. Chromatogr. B*, **2001**, *762*, 117.

19. Sung, W-C.; Huang, S-Y.; Liao, P-C.; Lee, G-B.; Li, C-W.; Chen, S-H. *Electrophoresis*, **2003**, *24*, 3648.

20. Hu, S.; Ren, X.; Bachman, M.; Sims, C. E.; Li, G.P.; Allbritton, *Anal. Chem.*, **2002**, *74*, 4117.

21. Lacher, N. A.; de Rooij, N. F.; Verpoorte, E.; Lunte, S. M.; *J. Chromatogr. A*, **2003**, *1004*, 225.

22. Ceriotti, L; de Rooij, N. F.; Verpoorte, E. *Anal. Chem.*, **2002**, *74*, 639.

23. Garcia, C. D.; Hadley, D. J.; Wilson, W. W.; Henry, C. S. *Biotechnol. Prog.*, **2003**, *19*, 1006.

24. Slentz, B. E.; Penner, N. A.; Lugowska, E.; Regnier, F. *Electrophoresis*, **2001**, *22*, 3736.

25. Slentz, B. E.; Penner, N. A.; Regnier, F. E. *J. Chromatogr. A*, **2002**, *948*, 225.

26. Hjertèn, S. *J.Chromatogr.*, **1985**, *347*, 191.

27. McDonald, J. C.; Duffy, D. C.; Anderson, J. R.; Chiu, D. T.; Wu, H.; Schueller, O. J. A.; Whitesides, G. M. *Electrophoresis*, **2000**, *21*, 27.

28. Makamba, H.; Kim, J. H.; Park, N.; Hahn, J. H. *Electrophoresis*, **2003**, *24*, 3607.

29. Chan, C.M. *Polymer Surface Modification and Characterization*; Hanser/Gardner Publications: Cincinnati, **1994**; Chapters 1,2,5.

30. Garbassi, F.; Morra, M.; Occhiello, E. *Polymer Surfaces*, 2nd Ed.; John Wiley and Sons: New York, **1998**; Chapters 2,6,7,12.

CHAPTER 6

CONCLUSIONS

The main goal of this dissertation was to explore new designs of porous monolithic sorbents for microscale separations.

As outlined in the introduction, the research was focus in two areas: i) the development of novel stationary phases with template porosity for capillary electrochromatography and ii) the investigation of monolith preparation in a channel on a microchip. In this section, the major conclusions drawn from the research in these areas are summarized.

The porosity of the polymeric stationary phase in monolithic columns is usually dictated by the nature and amount of the porogenic solvents employed. In this study, porous polymer monolithic capillary columns for liquid chromatography and capillary electrochromatography were prepared within the confines of fused-silica tubing using macromolecular compounds to affect porosity. The concept of pore templating is not new for our research group. Previously, silica beads were employed to template the porosity, and to a certain extent, to control the surface characteristics of polymer monoliths. A similar approached was used in this work. However, this time Starburst polyaminoamine (PAMAM) dendrimers (generation 4.5) in methanol were used as the porogen for the copolymerization of methacrylate-based monomers. Different column porosities were obtained by varying the amount of the dendrimer

template as evidenced by electron microscopy. The porous structure of the resulting monolith was shown to depend greatly on the dendrimer concentration. The effect of dendrimer concentration on chromatographic performance was also studied. It was found that the column efficiency and resolution increase with the dendrimer concentration reaching a maximum at 200 μM dendrimer. Higher concentrations of dendrimer produced large microglobules that affected the globule stacking and produced less uniform channels and thus lower separation efficiency. The separation of lysozyme tryptic digest fragments demonstrated the ability of these novel monolithic columns to separate complex mixtures.

Another goal of this research work was to explore novel approaches by which monolithic sorbents prepared inside the confines of a microchannel could be covalently attached to the inside walls of the channel.

Before attempting this objective, we probed the suitability of using voltage-driven separation techniques in chip formats. A glass microchip was used for this purpose. The results of this study showed that using a microchip electrophoresis system, rapid, efficient separations were obtained in a matter of minutes, even for very low concentrations of analytes. However, a major drawback of this technique is the detection system. While laser induced fluorescence is a highly sensitive detection method, only a small percentage of compounds fluoresce naturally. Therefore, the analytes must by derivatized prior to detection. One problem with such derivatization schemes is that analytes, like peptides or proteins, can become multiply labeled, therefore altering the separation.

The nature of microfluidic devices offers on exclusive opportunity to form a multiplexed and integrated system in one piece of chip.

Chip electrochromatography is an attractive option for lab-on-a-chip separations due to its separation performance and relative ease of implementation. Monolithic stationary phases appear to be the most versatile and robust type of stationary phases suitable for microchip formats. Monoliths stand out because of their large surface areas, simple preparation, and wide choice of surface chemistries. We demonstrated that they could also be readily adopted to a variety of substrate materials. Three different substrate materials were explored in this work: glass, poly(dimethylsiloxane) and polycarbonate. For each material, a method to facilitate wall-anchoring of the monolith was developed.

Our approach to prepare the monoliths was to functionalize the wall surface using [(methacryloxy)-propyl] trimethoxysilane. During the course of the subsequent polymerization, this surface modification will facilitate the covalent bonding of the porous monolith to the channel walls, thus anchoring and stabilizing the monolith.

For glass substrates, the preparation of the monolith followed a procedure developed for fabrication of capillary monolithic sorbents.

The possibility of using microchips made of plastic has also been explored. Plastic devices are attractive as they can be mass produced rapidly and inexpensively using replication technologies. We worked with two polymer substrates: poly(dimethylsiloxane) and polycarbonate.

Throughout this study, scanning electron micrograph images provided a closer look at the structure of the monolithic bed. These images proved that the monolith was indeed anchored to the wall of the microchannel.

In future, a significant advantage of the photoinitiation approach used in this study is the ability to define the size and location of the monolith using a mask through which the liquid polymerization mixture in the channel is irradiated. In this way, chips containing different separation matrixes to achieve multidimensional separation can be created.

Although much remains to be done, chip electrochromatography has a promising future in the development of μ-TAS. I believe that our approach opens new avenues that may help in the development of low-cost functional microdevices and systems for a variety of specific applications.